Article

Nearshore wave energy resource assessment for off-grid islands: A case study in Cuyo Island, Palawan, Philippines

Jonathan C. Pacaldo [1,2,3]* and Michael Lochinvar S. Abundo [1,2]*

[1] Center for Research in Energy Systems and Technology (CREST), University of San Carlos, Cebu city 6000, Philippines
[2] Engineering Graduate Program, School of Engineering, University of San Carlos, Cebu City 6000, Philippines
[3] Department of Electrical Engineering, Palawan State University, Puerto Princesa City 5300, Philippines
* Correspondence: 19103232@usc.edu.ph, mlabundo@usc.edu.ph

Abstract: Electrifying off-grid and isolated islands in the Philippines remains one of the challenges that hinders community development and one of the solutions seen to ensure energy security, energy access and promote low carbon future is the use of renewable energy sources. This study determines the nearshore wave energy resource during monsoon seasons in Cuyo Island using a 40-year wave hindcast and 9-year on-site wind speed data to develop high resolution wave energy model using SWAN wave model, and assessed its annual energy production through matching with wave energy devices. Results shows that average significant wave height (Hs), peak period (Tp) and wave power density (Pd) during northeast monsoon are Hs = 1.35 m, Tp = 4.79 s and Pd = 4.05 kW/m respectively, while southwest monsoon which is sheltered by the mainland resulted to a lesser outcome, Hs = 0.52 m, Tp = 3.37 s and Pd = 0.34 kW/m. While the simulated model was observed to overestimate the wave energy resource (Bias = 0.398, RMSE = 0.54 and SI = 1.34), it has a strong relationship with the observed values (average r = 0.9). Its annual energy production is highest at Station 5, with $AEP_{WaveBouy}$ = 43.761 MWh, $AEP_{Pelamis}$ = 216.786 MWh and $AEP_{Wave\ Dragon}$ = 2462.66 MWh.

Keywords: SWAN wave model; Nearshore wave energy resource assessment; Ocean renewable energy; Wave energy model simulation; Off-grid island electrification; Cuyo Island; Palawan

1. Introduction

Resource assessment is an important tool for verifying and quantifying energy resources, it serves as an initial step in the development of power supply operation. It is also essential in the characterization of the energy resource to support its development. In the Philippines, most off – grid island communities relies heavily on imported oils for its power generation needs [1], off-grids are normally the isolated island communities where it is impossible to be connected to the main grid. In 2018, 55.16% of installed capacity are coal and oil based, where coal alone shares 37.14% of this energy needs [2]. Although Philippines is an archipelagic country, it is up for the task of 100% electrification by 2040 for off-grid areas [3] most of this are isolated small island communities.

Wave energy development can be considered as one of the options in electrifying unviable island communities which cannot easily be reached by government programs because of its geographical constraints [4 - 7]. Quantifying wave energy resources in these areas will be the basis of further developing and promote renewable energy use and will also answer to the first three strategic directions of the energy sector in the country which are to ensure energy security, expand energy access and promote a low carbon future [3].

Several studies had already been done in assessing the Philippines wave energy resource. The recent study was conducted by Aminudin, Teh and Pacaldo (2021) [8] in

Dumaran Island, Palawan, which assessed the offshore wave energy resource of the island using 40–year hindcast data from MetOceanView. Quitoras, Abundo and Danao (2018) [9], assessed the energy flux of forty seven (47) coastal areas in the country and the result shows an energy flux of approximately 10–20 kW/m, this result is within the estimated global wave energy resource assessment as reported in [10 - 12]. Although the study covered a very large area, it does not include Palawan or any part of it or in particular, the Island of Cuyo. Another study conducted by the Mindanao State University showed that ocean energy in the country can provide an estimated 17,000 megawatts of electricity, and if we can tapped this energy, it would be of great help to mitigate the country's dependency in coal and imported oils as source of energy [13]. Also, a research group from Marine Science Institute and the College of Engineering of University of the Philippines started working together for the uptake of ocean renewable energy in the country by identifying potential sites for wave energy resource (Figure 1). Several spots had been identified in the part of Northern Palawan, those are, Calamian Group of Islands, Dumaran Group of Islands, Cuyo Group of Islands, Balabac and some parts of the Municipality of El Nido as a possible wave energy resource [14].

However, there are significant knowledge gap pertaining to quantification of nearshore wave energy climate and high resolution wave energy resource model on small islands in a semi-enclosed areas that can be used to develop wave energy project. Having sufficient information regarding wave energy resource potential for this specific type of islands in the Philippines will paved way for an in-depth development or device solution for small scale wave energy production to support the island's power requirements.

Here, a high resolution nearshore wave model was developed through (Simulating Wave Nearshore) SWAN wave model, a third generation numerical wave model, by using a 40-year wave hindcast from MetOceanView (1978 – 2018) [15] and 9 – year (2010 – 2018) on-site measurement of wind speed and wind direction at Philippine Atmospheric, Geophysical, and Astronomical Services Administration (PAGASA) Cuyo Station [16]. The SWAN wave model was used to analyse the seasonal and spatial variability of the island's wave climate. To determine the annual energy production, a calculation was made by matching a suitable type of wave energy device that optimizes the wave energy resource on selected stations.

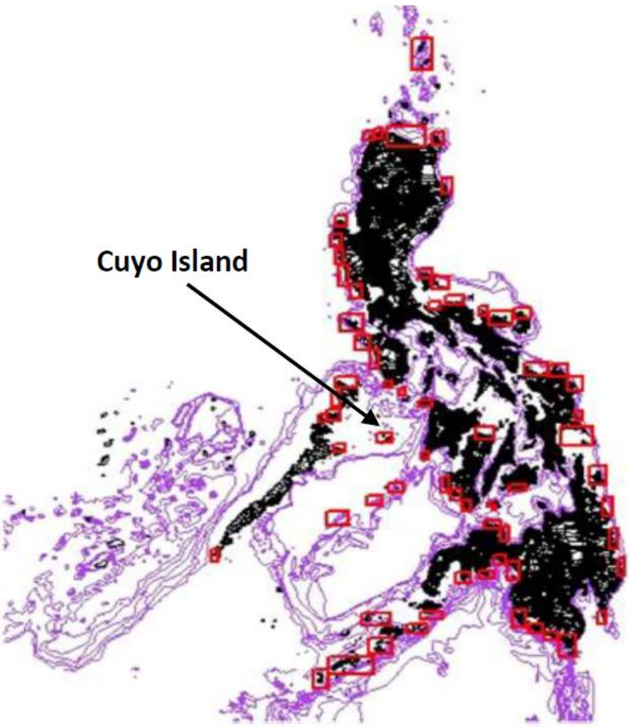

Figure 1. Probable Sites for wave energy in the Philippines identified by University of the Philippines Marine Science Institute.

2. Materials and Methods

2.1 Study Area

Cuyo Island is the largest island among the 45 islands under Cuyo Archipelago, about 278.37 km north-east of Puerto Princesa City, Palawan and has a land area of 57 km^2 (22 $mi.^2$) (Figure 2). It has an estimated population of 34,556 (2015 CENSUS) which is about 4.04% of the total population of Palawan Province [17, 18]. The island was identified to have a good to excellent wind resource and the average wind speed measured for 30 years was 5 m/s at 4 meters elevation [19], given this, a potential wave energy resource as suggested in [14] is highly probable. There are three cases in which wave is propagated, one (1) a large storm generates deep water waves that propagate across shallower water while the waves continue to grow due to wind, two (2) a large storm generates winds in an area remote from the site of interest and as waves cross shallower water with negligible wind, they propagate to the site as swell, and lastly, three (3) Wind blows over an area of shallow water generating waves that grow so large as to interact with the bottom [20], this indicates that the island characteristic satisfies case number three (3), a good wind resource plays a significant role in wave transformation.

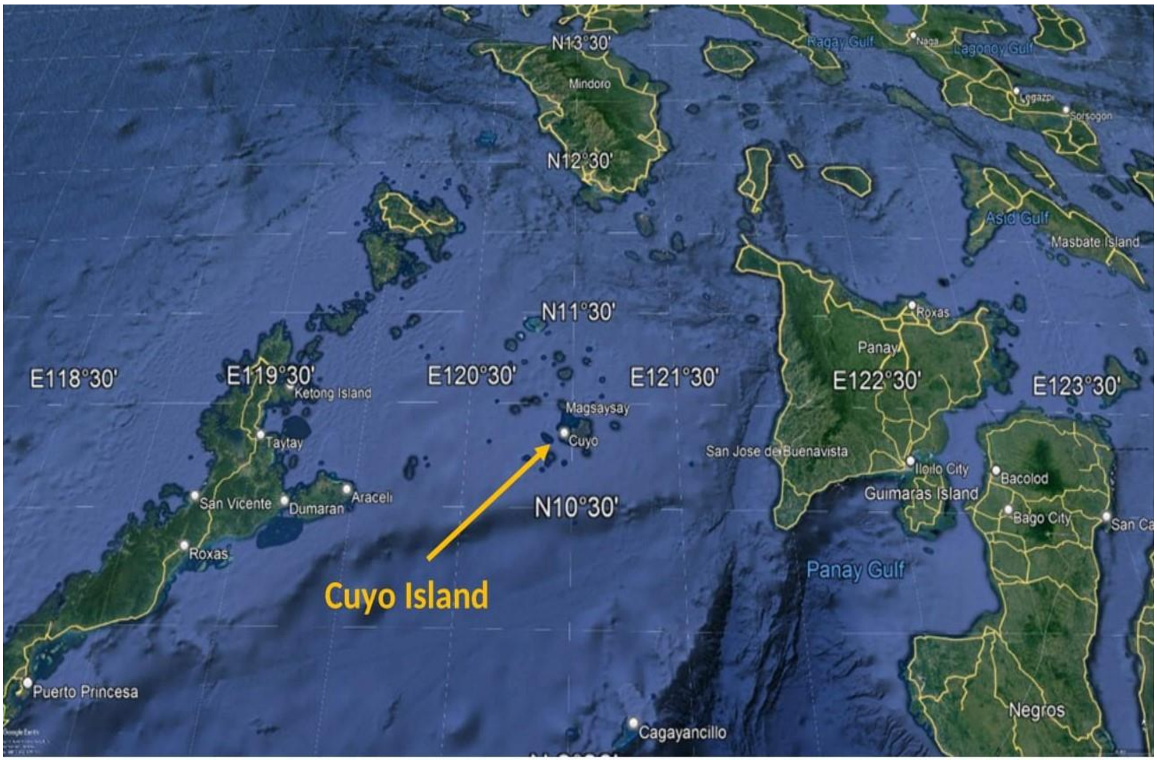

Figure 2. Map showing Cuyo Island at the Northeastern part of Palawan (10.51 N Lat., 121.04 E Long.)

2.2 40 – year wave hindcast dataset (1978 – 2018)

To describe the wave climate in Cuyo Island, a wave model was developed using SWAN wave model and will be using MetOceanView's 40-year, 3-hourly interval wave hindcast dataset (1978 – 2018) as initial condition and to describe the wave climate surrounding the island, this is a high resolution web-based weather forecasting developed by MetOcean Solutions in New Zealand using Ltd WW3 Tolman Chalicov (MSL WW3 TC) wave model [9]. Several studies using MetOcean Solutions had been published in different fields of study, such as, techno-economic assessment of wave energy [9], wave energy resource assessment [20], optimizing hybrid diesel – wave electrical system for an off-grid island [21], weather forecasting for marine operations [22] and marine weather monitoring [23]. For this study, nine (9) stations surrounding Cuyo Island are selected (Figure 3) for descriptive statistical analysis and among these stations, four (4) are selected (stations 4, 8, 12, and 14) that will serve as initial condition to simulate numerical wave model during Northeast and Southwest Monsoon and further determine the wave energy resource nearer to the island (Figure 4).

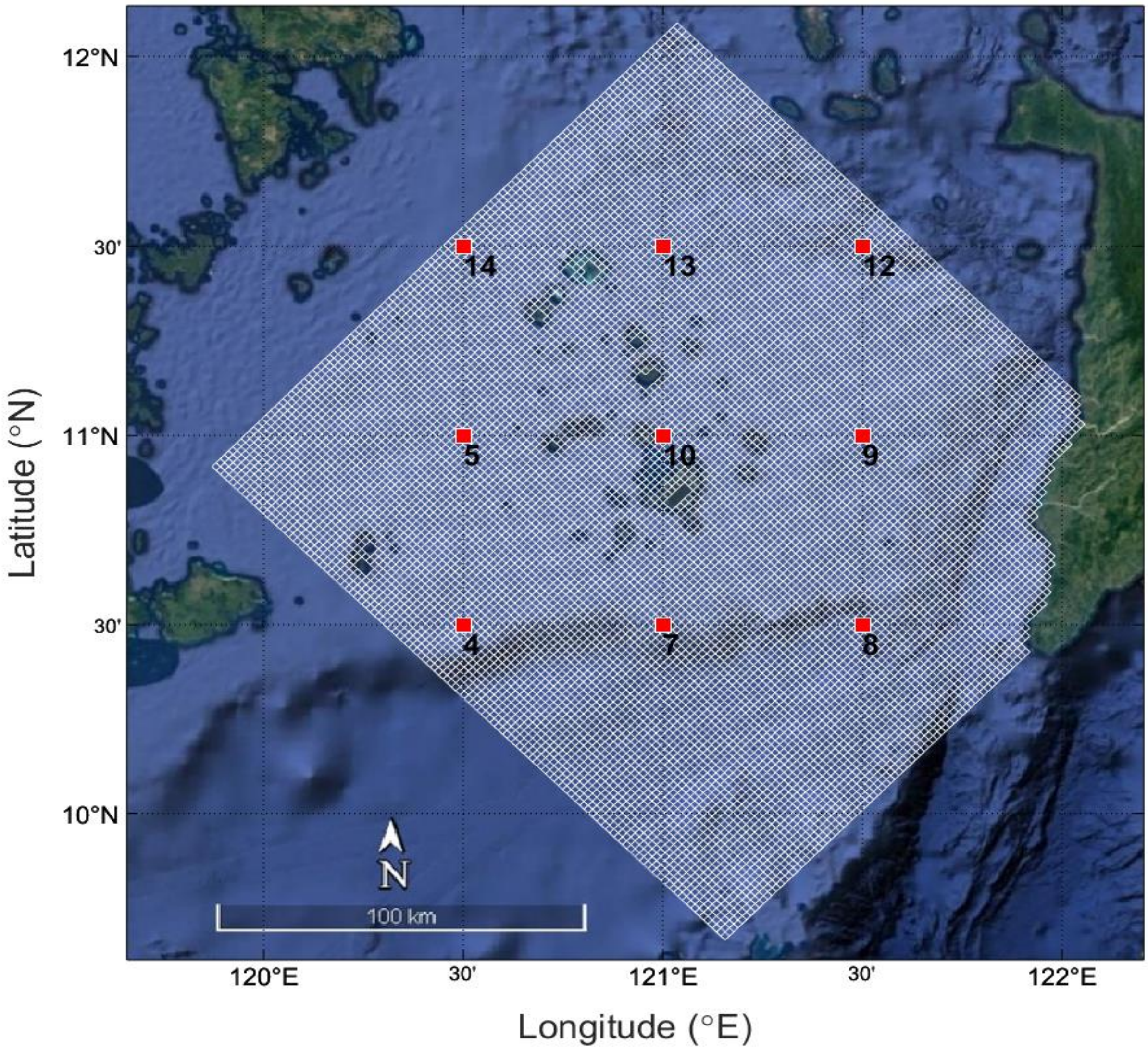

Figure 3. Cuyo Island showing the 9 stations of MetOceanView's 40-year hindcast wave data (Station - 4, 10.5 N Lat., 120.5 E Long, Station - 5, 11.0 N Lat., 120.5 E Long., Station 7 – 10.5 N Lat., 121.0 E Long., Station – 8, 10.5 N Lat., 121.5 E Long., Station – 9, 11.0 N Lat., 121.5 E Long., Station – 10, 11.0 N Lat., 121.0 E Long., Station 12 – 11.5 N Lat., 121.5 E Long., Station – 13, 11.5 N Lat., 121.0 E Long., Station – 14, 11.5 N Lat., 120.5 E Long.)3. Results

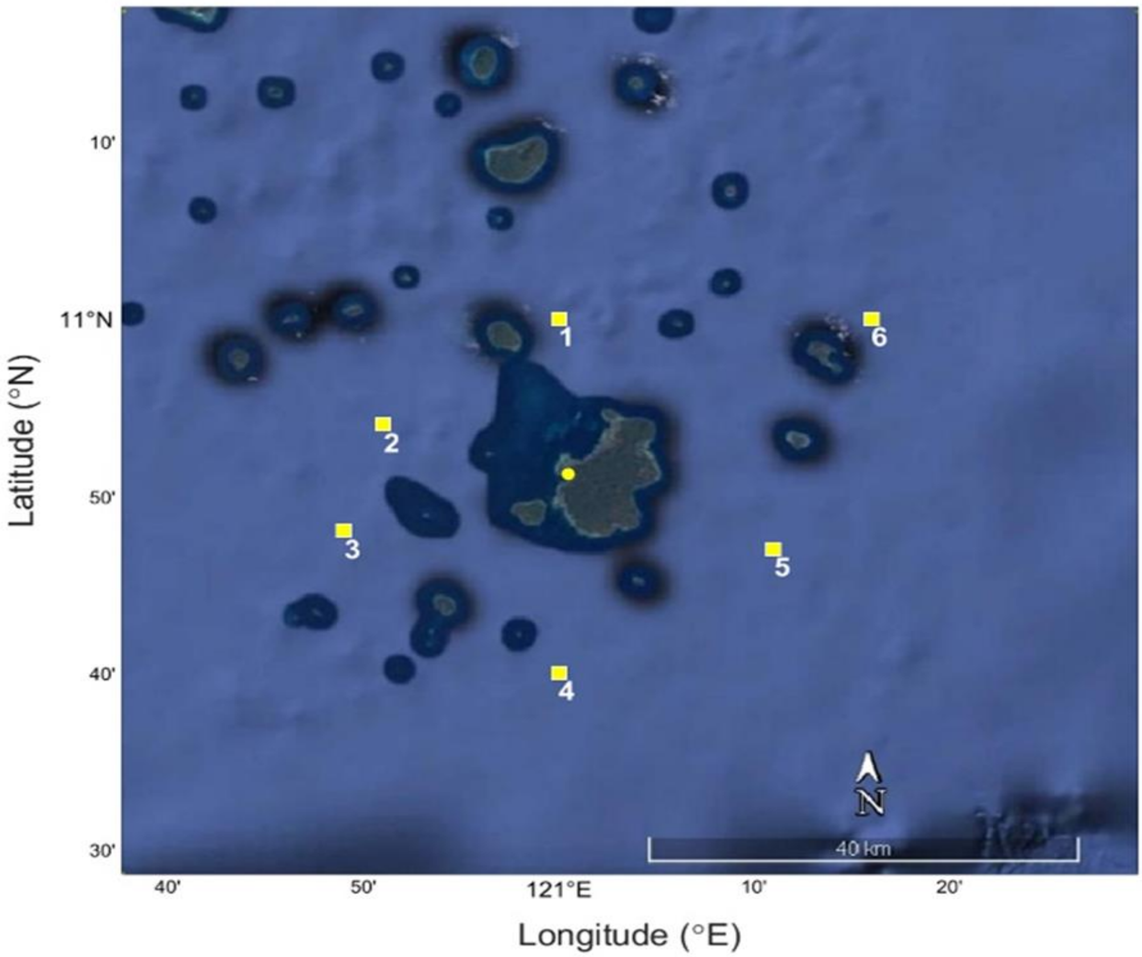

Figure 4. Sites generated through SWAN wave model (Station – 1, 11.0 N Lat., 121.0 E Long., Station – 2, 10.85 N Lat., 120.8 E Long., Station – 3, 10.70 N Lat., 120.70 E Long., Station – 4, 10.5 N Lat., 121.0 E Long., Station – 5, 10.8 N Lat., 121.30 E Long., Station – 6, 11.0 N Lat., 121.30 E Long.)

2.3 Directional wave height scenario

This study focused on the nearshore wave energy resource of the island and the nearest data set that best describe the directional wave behaviour nearshore is the 9-year (2010 – 2018) PAGASA - Cuyo Station wind speed and wind direction data set and Station 10 which is 15 km away from the island and has an annual significant wave height of 1.2 m and annual wave power density of 3.13 kW/m [21]. The directional wave height is presented using wind rose and wave rose diagram, a rose diagram represents two dimensional orientation of the wind and wave climate that represents the relative frequencies of different wind and wave directions and so as the wind and wave heights over a period of time. It displays the distribution of data in a way that can be easily understood and evaluated [24]. Figure 5 shows the wave rose diagram of the 40-year hindcast at station 10, wave data are taken every five (5) years starting from 1978 to 2018 at Station 10. Dominant wave directions are consistent and are coming from the north-eastern and south-western side of the island. This is mainly due to northeast monsoon which is typically from the months of December – February and southwest monsoon from the months of June – August. The directional wave height scenario is consistent with the nine (9) – year on-site wind measurement from 2010 – 2018 by the PAGASA – Cuyo Station as shown in Figure 6. Table 1 shows a high correlation (r = 0.75) between the hindcast wave data and the on-site wind measurement.

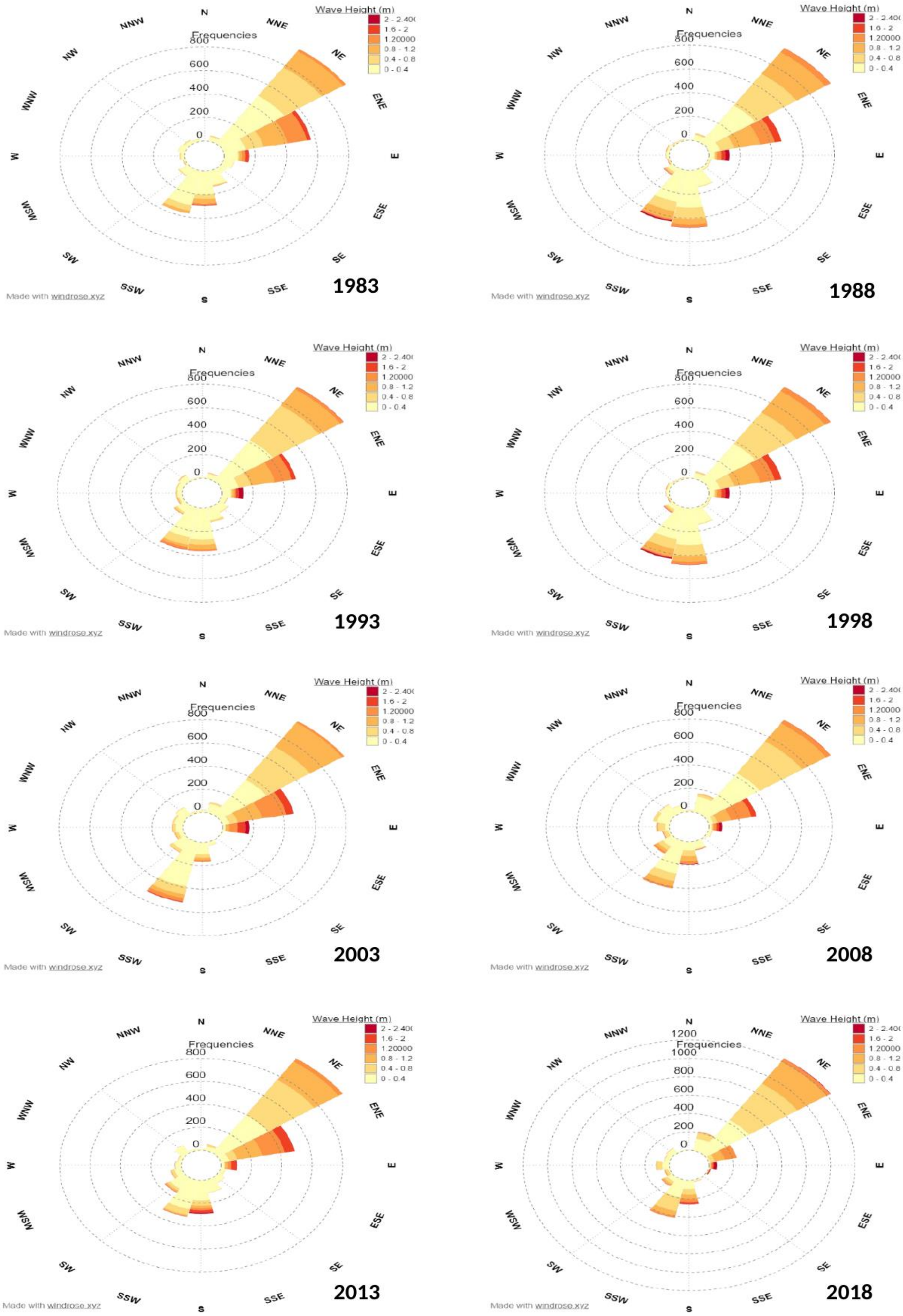

Figure 5. Wave rose diagram at station 10 (11.0 N Lat., 121.0 E Long.) having a 5-year interval (Data source - MetOceanView)

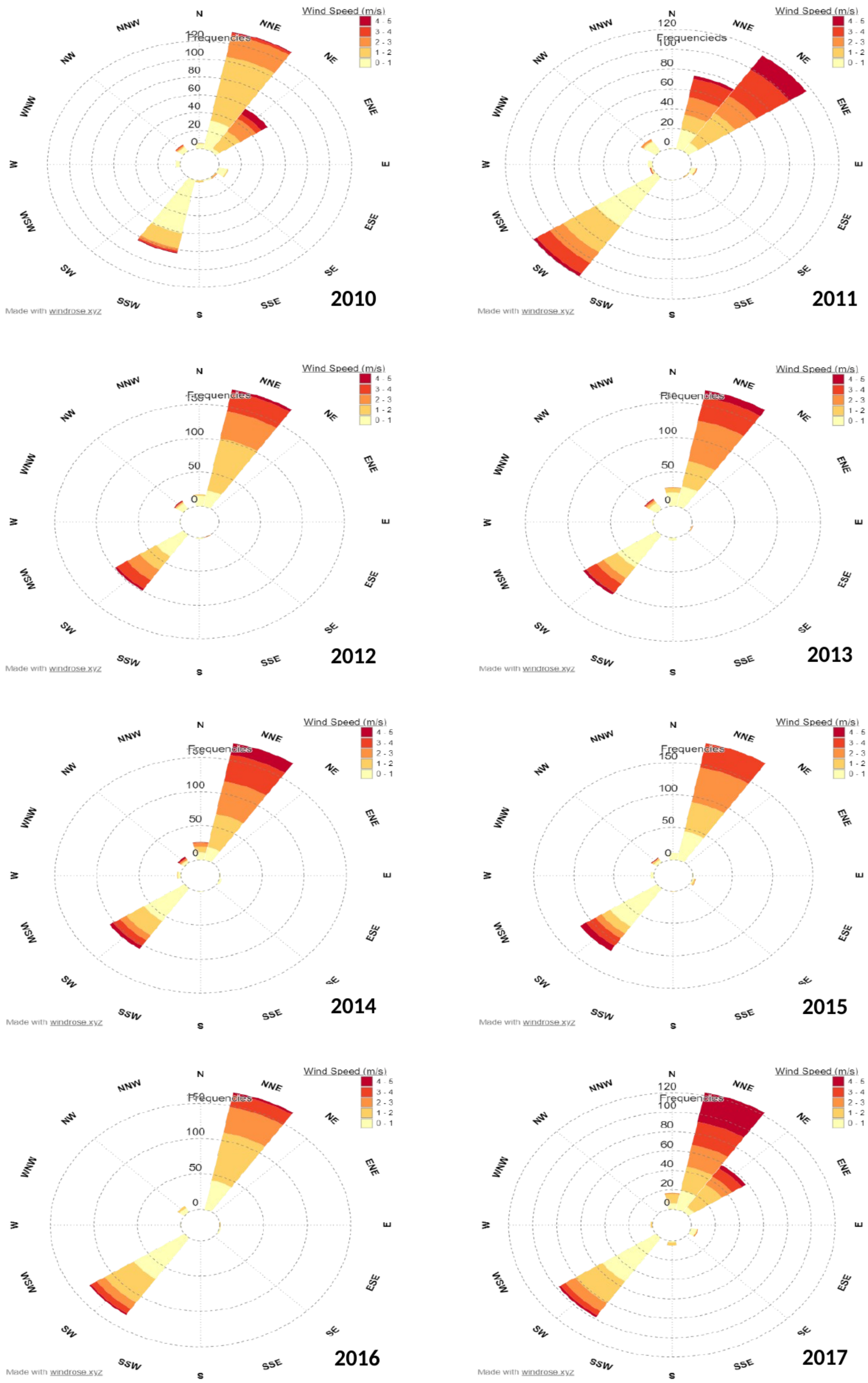

Figure 6. . Wind Rose diagram of PAGASA Cuyo Station (10.85 N Lat., 121.04 E Long.) from 2010 – 2017.

Table 1. Correlation between MetOceanView wave height data to PAGASA measured wind speed

MetOceanView Station	Distance from Cuyo Island (km)	Wave Height (MetOceanView) vs Wind Speed (PAGASA Cuyo Station)	Wind Speed (MetOceanView) vs Wind Speed (PAGASA Cuyo Station)	Annual Significant Wave Height, Hs (m)	Annual Wave Power Density (kW/m)
4	68	0.71	0.73	1.34	4.28
5	60	0.76	0.77	1.44	5.00
7	40	0.60	0.60	1.11	2.66
8	66	0.51	0.57	1.17	3.06
9	56	0.66	0.62	1.16	3.05
10	15	0.75	0.75	1.20	3.13
12	92	0.75	0.74	1.38	4.25
13	72	0.73	0.76	1.44	4.88
14	92	0.62	0.69	1.40	4.88

2.4 Validation

To validate the accuracy of the resulting wave model, statistical analysis between the model result and the observe values will be calculated using the following statistical metrics or error statistics:

$$\text{Mean of measured } (\bar{X}) \text{ parameters; } \bar{X} = \frac{1}{n}\sum x_i \ , \tag{1}$$

$$\text{Mean of hindcast } (\bar{Y}) \text{ parameters; } \bar{Y} = \frac{1}{n}\sum y_i \ , \tag{2}$$

$$\text{Bias; } = \frac{1}{n}\sum(y_i - x_i) \ , \tag{3}$$

$$\text{Root Mean Square Error; } SE = \sqrt{\frac{1}{n}\sum(x_i - y_i)^2} \ , \tag{4}$$

$$\text{Scatter Index; SI} = \frac{RMSE}{\bar{X}} \ , \tag{5}$$

$$\text{Pearson's Correlation Coefficient; } r = \frac{\sum(x_i - \bar{X})(y_i - \bar{Y})}{\sqrt{\sum(x_i - \bar{X})^2 \sum(y_i - \bar{Y})^2}} \ , \tag{6}$$

Here, x_i is the significant wave height of the observed values, y_i is the significant wave height hindcast from the wave model and n is total values for both parameters.

The observed parameters are from the 2018 wind data from PAGASA - Cuyo Station processed into its equivalent significant wave heights through SWAN wave model, the processed data were taken in a 1-hour interval. The hindcast parameters are the simulated significant wave heights in stations 1 -6 with the same interval. The Bias represents the model's mean long-term error, where a positive value means an average overestimation or underestimation if the value is negative as compared to the measurements. Root Mean Square Error or RMSE is the residuals standard deviation or the estimated error between the model predictions and measured observations, where larger numbers means a greater variance. Scatter Index (SI) presents the percentage of RMSE difference with respect to mean observation or is a normalized measure of error where lower values indicates a better model performance. The Pearson correlation coefficient r, is a measure of the degree of linear dependence or relationship between the model and the observations [25].

2.5 SWAN wave model

This study was undertaken to understand the wave characteristics in Cuyo using MetOceanView's wave hindcast data, PAGASA wind data, and Simulating Waves Nearshore (SWAN) wave model. The MetOceanView data were used in hindcasting deep-water offshore wave conditions and describing the wave climate in the area in terms of peak wave direction and period, and significant wave heights. SWAN wave models were simulated to describe wave characteristics as it approaches the coastal areas of Cuyo during the Northeast and Southwest Monsoon.

SWAN wave model is a third generation full spectral wave model based on the action balance equation (Equation 1) that simulates realistic estimates of wave parameters such as, short-crested waves in coastal areas, lakes and estuaries from a given wind, bottom, and current conditions [25, 26]. SWAN wave model is based on Eulerian formulation discrete spectral balance of action density that accounts for refractive propagation over arbitrary bathymetry and current fields [26]. SWAN model describes the wave climate by means of action density N (σ, θ) instead of energy density E (σ, θ).

$$\frac{\partial N}{\partial t} + \frac{\partial c_x N}{\partial x} + \frac{\partial c_y N}{\partial y} + \frac{\partial c_\sigma N}{\partial \sigma} + \frac{\partial c_\theta N}{\partial \theta} = \frac{S_{tot}}{\sigma} \quad (7)$$

The first term on the left-hand side of the equation stands for the change of action density in time, the second and third term represents the propagation velocities in x and y axis. The fourth and fifth term represents shifting of relative frequency with respect to the variations in depths and currents and refraction induced by depth and currents respectively. The right-hand side of the action balance equation represents the source term in terms of energy density, representing the effects of generation, dissipation and nonlinear wave-wave interactions [26].

SWAN wave model was used in different wave resource assessment projects, it was coupled with WAVEWATCH III to determine the wave energy resource along the Northern Spanish coast, the model was validated with buoy data to evaluate the its accuracy and presented statistical analysis of wave parameters and wave power results [27], the same method was used to determine the nearshore wave energy resource in Canary islands [6] and in Sicily, Italy [28], in China, SWAN wave model coupled with Finite-Volume Community Ocean Model (FVCOM) was employed to simulate waves and currents during Typhoon Fung-wong (2014) and Typhoon Chan-hom (2015) around the Zhoushan Islands [29], in Puerto Rico and the United States of Virgin Islands, SWAN wave model was used to simulate the nearshore wave energy resource for a possible wave power generation in the US Caribbean [30].Through the years, analysing wave behaviour and wave resource assessment, SWAN wave model was utilized either coupled with another wave model tool or utilized alone, to answer and analysed wave parameters on nearshore areas, some of which are Madiera Islands in Portugal [31], Long Island in New York [32], Hawaiian Islands [33], Azores Islands [34], Cape Verde Islands [35], Persian Gulf [36], South China Sea [37], Sardinia Island [38], Gulf of Thailand [39], Cornish (UK) [40], Atlantic coast of France [41], Scotland [42, 43], Chile [44], Australia [45], and Tenerife Island in Spain [4].

In this study, a nested model was used to provide the necessary boundary conditions for the Cuyo wave model. The coarse grid is a rectangular 110 x 120 grid with ~1.5km resolution, rotated 45° to align the grid with the dominant wind and wave directions due to the northeast (NE, Amihan) and southwest (SW, Habagat) monsoons (Figure 7, white grid). On the other hand, the nested, high-resolution grid is a 123 x 93 rectangular grid with ~500m resolution and focused on the east side of the Cuyo Archipelago (Figure 7, blue grid). Subsequently, downloaded bathymetric data from GEBCO2021 [46] with 450m resolution were also interpolated onto the model grid (Figure 8).

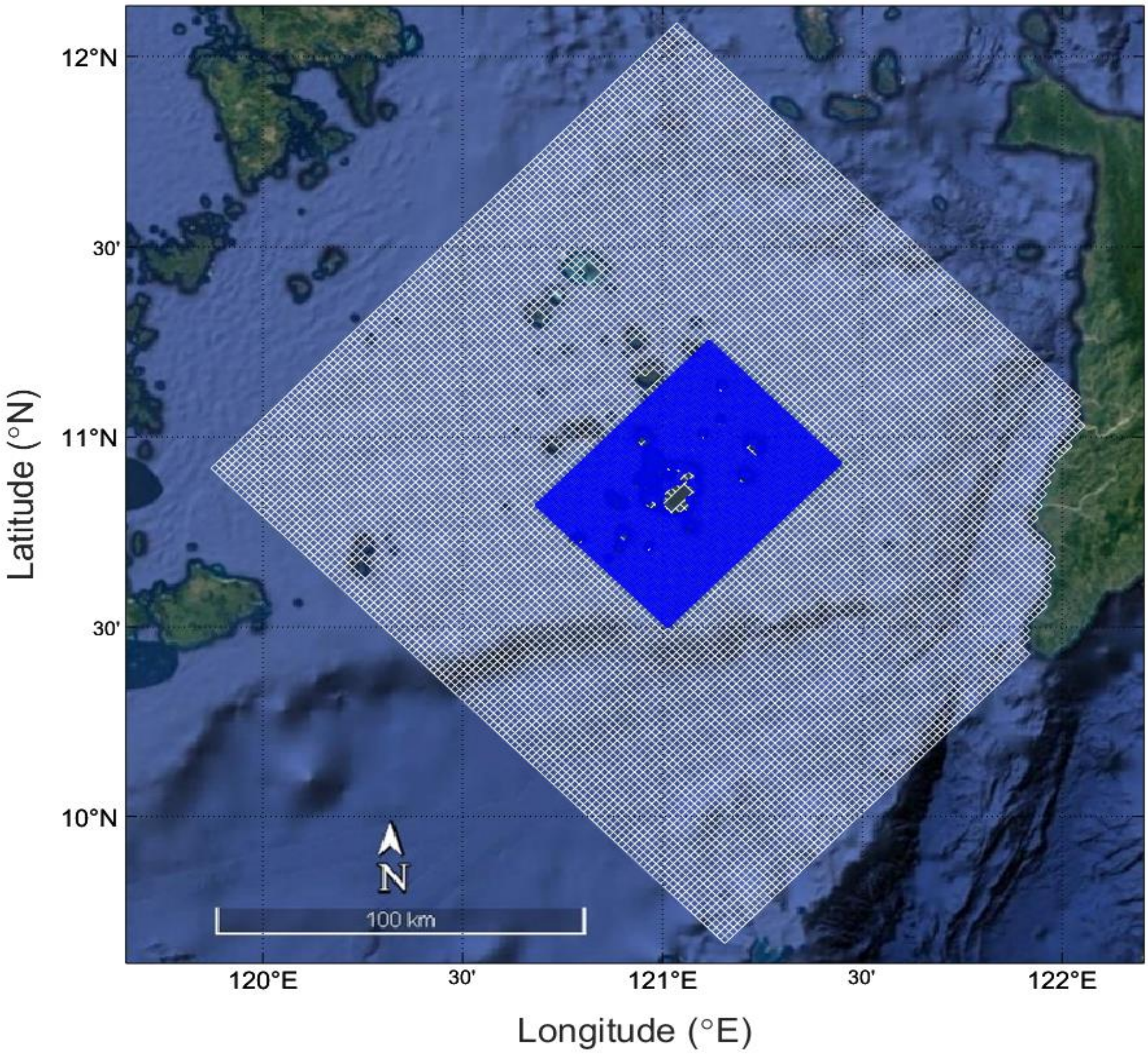

Figure 7. Nested grids (white for coarse grid, blue for fine grid) used for the SWAN wave models.

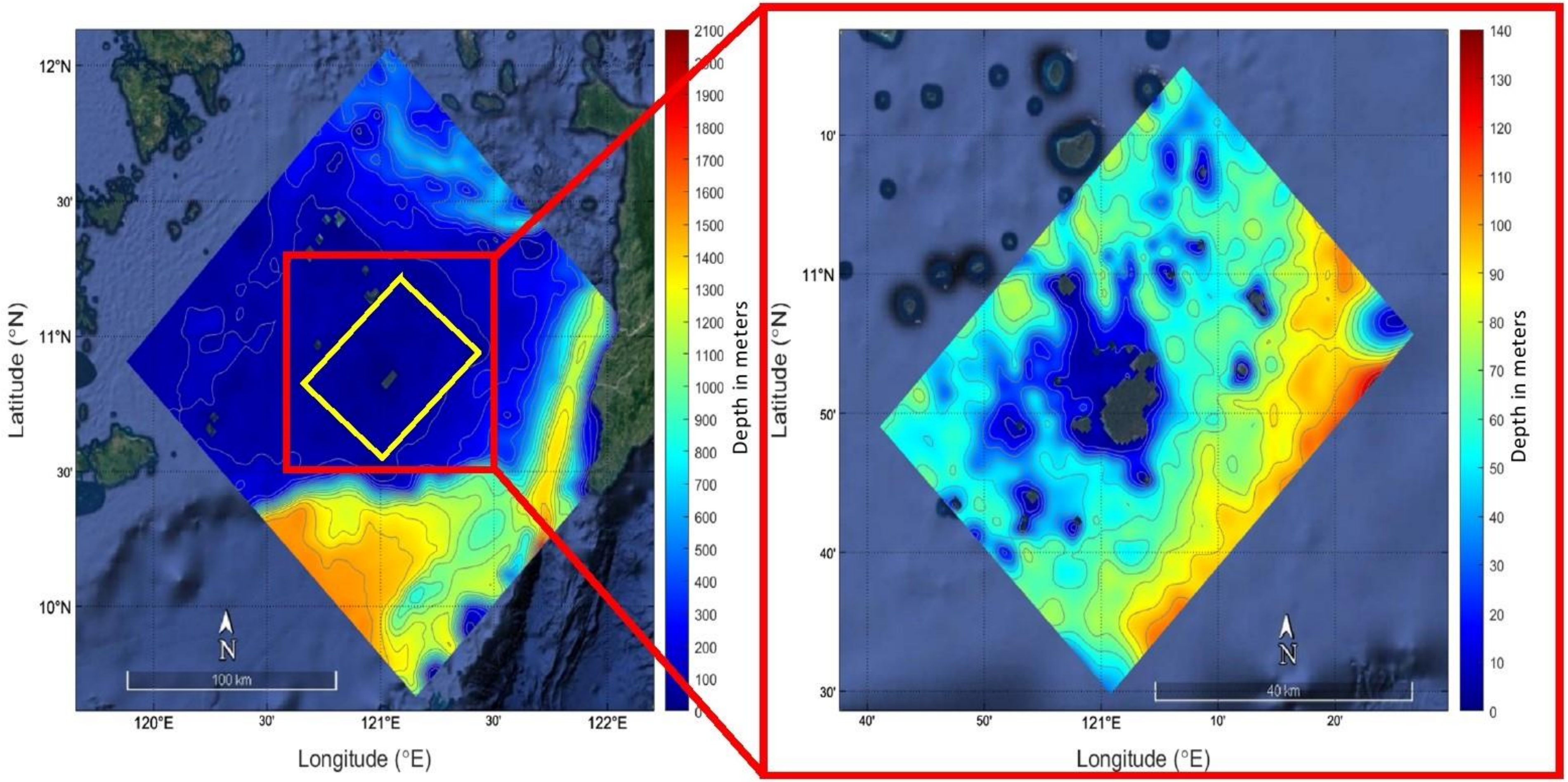

Figure 8. Downloaded GEBCO bathymetric data (adjusted to positive values in meters for Delft3d compatibility) interpolated onto the coarse (left panel) and fine (right panel) grid of the SWAN model. Red is deepest and blue is shallowest. Contour intervals for coarse grid (left panel) is every 100m depth while it's every 10m depth for fine grid (right panel).

Four simulations were performed to represent the NE and SW monsoon wave conditions. The boundary and wave conditions (significant wave height, and peak wave direction and period were assumed uniform along the specific boundary orientation) inputted into the model runs were based on the computed mean of 3-hourly MetOceanView 2008-2018 data (Table 2) taken from the following stations (Figure 9):

- Station 4 (southwest boundary orientation) at 10.5°N and 120.5°E,
- Station 8 (southeast boundary orientation) at 10.5°N and 121.5°E,
- Station 12 (northeast boundary orientation) at 11.5°N and 121.5°E, and
- Station 14 (northwest boundary orientation) at 11.5°N and 120.5°E.

Table 2. Mean significant wave height (Hs), peak period (Tp) and direction (Dp) from MetOceanView 2008-2018 data for the northeast (Decembe-January-February (DJF)/Amihan) and southwest (June-July-August (JJA)/Habagat) monsoon.

Station	DJF mean (Amihan)			JJA mean (Habagat)		
	Hs	Tp	Dp	Hs	Tp	Dp
4	1.1131	5.2592	46.6263	0.5066	4.1881	-167.453
8	0.8601	4.8991	28.2988	0.5044	4.2172	-150.142
12	1.106	4.8461	38.0907	0.4972	4.3267	-153.027
14	1.1139	5.3135	62.773	0.4829	4.4801	-164.637

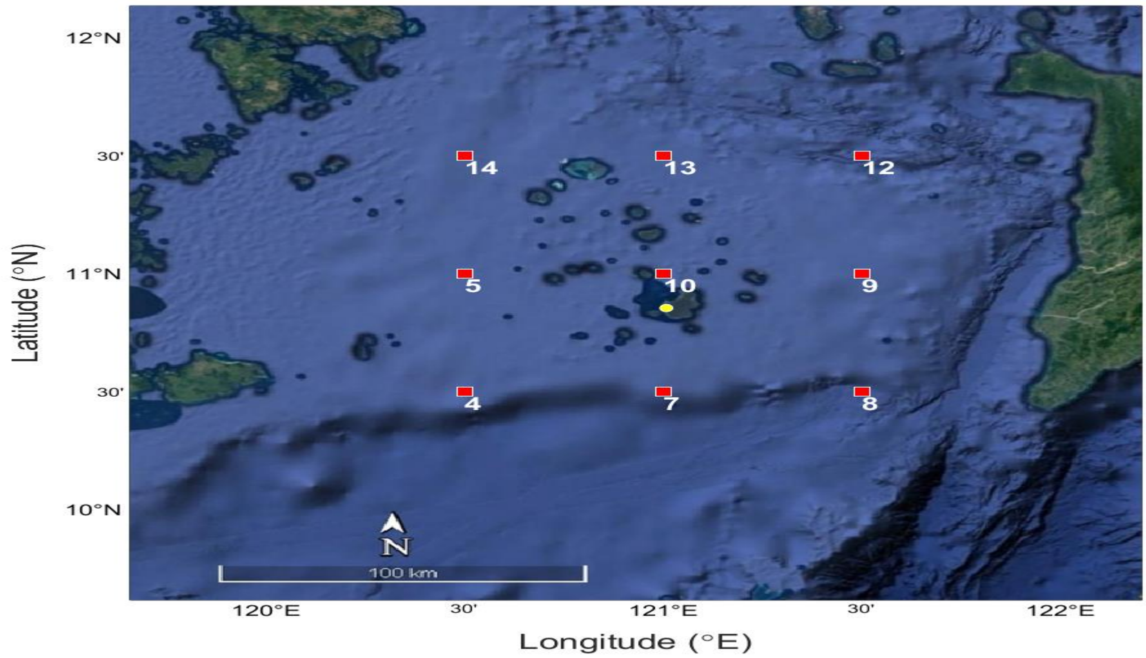

Figure 9. Map of MetOceanView stations (red squares) where 3-hourly data on wind velocity, significant wave height, and peak wave direction and period were extracted. On the other hand, the yellow circle is the PAGASA Cuyo Station where daily wind data was recorded.

Additionally, the following parameter settings were applied in the wave model:

- *Wave spectrum*
    - At the wave model boundary, a JONSWAP spectrum with a peak enhancement factor of 3.3 was assumed.
    - Similarly, a directional spreading of approximately 25ºdeg (power function, with power = 4) was assumed.
- *Physical parameters*
    - Third-generation mode for wind growth, quadruplet interactions and white-capping[1] [47] were considered.
    - Constant depth induced breaking (Alpha = 1[2], Gamma= 0.73[3])
    - Constant JONSWAP bottom friction (friction coefficient = 0.067 m^2/s^3)[4] [48]
    - Non-linear wave-wave interactions due to the triads were not considered.
    - No diffraction
- *Numerical parameters*
    - The amount of diffusion of the implicit scheme in the directional space (through Directional Discretization parameter) and frequency space (through the Frequency Discretization) were set to the default value 0.5.
    - Accuracy:
        - Relative change H_s-T_{m01}: 0.02
        - Relative change with respect to the mean value: 0.02 for both H_s and T_{m01}
        - Convergence percentage of wet grid points: 98%
        - Maximum number of iterations: 15

2.6 Annual energy generation

Annual energy generated was computed using the stations wave scatter diagram and wave energy devices power matrix using the formula given in equation 8 [9]. Wave scatter diagram is the condition of sea state at a particular location in a year which is generated from the historical data (Table 3 – 8), while the wave energy converters (WEC) power matrix is the actual amount of available energy the device can capture (Table 9 – 11). This study adopted the wave energy devices use in [9] for Philippines settings, the wave dragon (4000 kW), Pelamis (750 kW) and WaveBouy (250 kW) to determine the possible annual energy that can be utilized per stations [9, 49, 50].

Annual Energy Production in MWh (AEP) = Wave Scatter Diagram (in hours)*Power matrix(MW) (8)

Table 3. Wave Scatter Diagram, in hours at Station 1

---

[1] Based on (Komen, Hasselmann, & Hasselmann, 1984) [47]

[2] The coefficient for determining the rate of dissipation.

[3] The value of the breaker parameter defined as H_m0/d.

[4] The bottom friction is computed based on the empirical model of JONSWAP (Hasselmann, et al., 1973) [48]. The coefficient of the JONSWAP formulation is set at 0.067 m^2/s^3, which is a typical default value for wind sea conditions.

Wave Scatter Diagram													
Station 1		Period (Tp), seconds											
		0	1	2	3	4	5	6	7	8	9	10	11
		1	2	3	4	5	6	7	8	9	10	11	12
Wave height (Hs), meters 0	1	150	1155	2178	2682	30	3	▪	3	▪	3	3	▪
1	2	▪	▪	▪	174	1587	384	▪	▪	▪	▪	▪	▪
2	3	▪	▪	▪	▪	▪	207	114	▪	▪	▪	▪	▪
3	4	▪	▪	▪	▪	▪	▪	51	306	▪	▪	▪	▪
4	5	▪	▪	▪	▪	▪	▪	▪	2	▪	▪	▪	▪

Table 4. Wave Scatter Diagram, in hours at Station 2

Wave Scatter Diagram													
Station 2		Period (Tp), seconds											
		0	1	2	3	4	5	6	7	8	9	10	11
		1	2	3	4	5	6	7	8	9	10	11	12
Wave height (Hs), meters 0	1	147	1149	2139	2730	78	9	▪	3	▪	▪	3	3
1	2	▪	▪	▪	234	1587	315	▪	▪	▪	▪	▪	▪
2	3	▪	▪	▪	▪	▪	255	54	▪	▪	▪	▪	▪
3	4	▪	▪	▪	▪	▪	▪	27	▪	▪	▪	▪	▪
4	5	▪	▪	▪	▪	▪	▪	▪	▪	▪	▪	▪	▪

Table 5. Wave Scatter Diagram, in hours a Station 3

Wave Scatter Diagram													
Station 3		Period (Tp), seconds											
		0	1	2	3	4	5	6	7	8	9	10	11
		1	2	3	4	5	6	7	8	9	10	11	12
Wave height (Hs), meters 0	1	147	1194	2178	2790	75	9	3	▪	3	▪	3	3
1	2	▪	▪	▪	231	1569	276	▪	▪	▪	▪	▪	▪
2	3	▪	▪	▪	▪	▪	210	48	▪	▪	▪	▪	▪
3	4	▪	▪	▪	▪	▪	▪	21	▪	▪	▪	▪	▪
4	5	▪	▪	▪	▪	▪	▪	▪	▪	▪	▪	▪	▪

Table 6. Wave Scatter Diagram, in hours at Station 4

Wave Scatter Diagram													
Station 4		Period (Tp), seconds											
		0	1	2	3	4	5	6	7	8	9	10	11
		1	2	3	4	5	6	7	8	9	10	11	12
Wave height (Hs), meters 0	1	147	1050	2106	2628	108	9	3	3	▪	▪	3	3
1	2	▪	▪	▪	105	1704	465	▪	▪	▪	▪	▪	▪
2	3	▪	▪	▪	▪	▪	237	132	▪	▪	▪	▪	▪
3	4	▪	▪	▪	▪	▪	▪	36	21	▪	▪	▪	▪
4	5	▪	▪	▪	▪	▪	▪	▪	▪	▪	▪	▪	▪

Table 7. Wave Scatter Diagram, in hours at Station 5

Wave Scatter Diagram													
Station 5		Period (Tp), seconds											
		0	1	2	3	4	5	6	7	8	9	10	11
		1	2	3	4	5	6	7	8	9	10	11	12
Wave height (Hs), meters													
0	1	147	1017	1944	2643	99	9	3	3	▪	3	▪	3
1	2	▪	▪	▪	69	1776	531	▪	▪	▪	▪	▪	▪
2	3	▪	▪	▪	▪	▪	258	165	▪	▪	▪	▪	▪
3	4	▪	▪	▪	▪	▪	▪	51	24	▪	▪	▪	▪
4	5	▪	▪	▪	▪	▪	▪	▪	15	▪	▪	▪	▪

Table 8. Wave Scatter Diagram, in hours at Station 6

Wave Scatter Diagram													
Station 6		Period (Tp), seconds											
		0	1	2	3	4	5	6	7	8	9	10	11
		1	2	3	4	5	6	7	8	9	10	11	12
Wave height (Hs), meters													
0	1	150	1020	1920	2697	132	6	3	3	▪	3	▪	3
1	2	▪	▪	▪	51	1710	567	▪	▪	▪	▪	▪	▪
2	3	▪	▪	▪	▪	▪	252	147	▪	▪	▪	▪	▪
3	4	▪	▪	▪	▪	▪	▪	60	21	▪	▪	▪	▪
4	5	▪	▪	▪	▪	▪	▪	▪	15	▪	▪	▪	▪

Table 9. Power matrix, in kW of AquaBouy

Power Matrix, AquaBouy		Period, in seconds											
		5	*6*	*7*	*8*	*9*	*10*	*11*	*12*	*13*	*14*	*15*	*16*
		6	*7*	*8*	*9*	*10*	*11*	*12*	*13*	*14*	*15*	*16*	*17*
Wave Height, in meters													
0	*1*	▪	**8**	**11**	**12**	**11**	**10**	**8**	**7**	▪	▪	▪	▪
1	*1.5*	**13**	**17**	**25**	**27**	**26**	**23**	**19**	**15**	**12**	**12**	**12**	**7**
1.5	*2*	**24**	**30**	**44**	**49**	**47**	**41**	**34**	**28**	**23**	**23**	**23**	**12**
2	*2.5*	**37**	**47**	**69**	**77**	**73**	**64**	**54**	**43**	**36**	**36**	**36**	**19**
2.5	*3*	**54**	**68**	**99**	**111**	**106**	**92**	**77**	**63**	**51**	**51**	**51**	**27**
3	*3.5*	▪	**93**	**135**	**152**	**144**	**126**	**105**	**86**	**70**	**70**	**70**	**38**
3.5	*4*	▪	▪	**122**	**176**	**198**	**188**	**164**	**137**	**112**	**112**	**112**	**49**
4	*4.5*	▪	▪	**223**	**250**	**239**	**208**	**173**	**142**	**115**	**115**	**115**	**62**
4.5	*5*	▪	▪	**250**	**250**	**250**	**250**	**214**	**175**	**142**	**142**	**142**	**77**
5	*5.5*	▪	▪	**250**	**250**	**250**	**250**	**250**	**211**	**172**	**172**	**172**	**92**

Table 10. Power Matrix, in kW of Pelamis

Power Matrix, Pelamis			Period, in seconds																
			4.5	5	5.5	6	6.5	7	7.5	8	8.5	9	9.5	10	10.5	11	11.5	12	12.5
			5	5.5	6	6.5	7	7.5	8	8.5	9	9.5	10	10.5	11	11.5	12	12.5	13
Wave Height, in meters	0	0.5	▪	▪	▪	▪	▪	▪	▪	▪	▪	▪	▪	▪	▪	▪	▪	▪	▪
	0.5	1	▪	22	29	34	37	38	38	37	35	32	29	26	23	21	▪	▪	▪
	1	1.5	32	50	65	76	83	86	86	83	78	72	65	59	53	47	42	37	33
	1.5	2	57	88	115	136	148	153	152	147	138	127	116	104	93	83	74	66	59
	2	2.5	89	138	180	212	231	238	238	230	216	199	181	163	146	130	116	103	92
	2.5	3	129	198	260	305	332	340	332	315	292	266	240	219	210	188	167	149	132
	3	3.5	▪	270	354	415	438	440	424	404	377	362	326	292	260	230	215	202	180
	3.5	4	▪	▪	462	502	540	546	530	499	475	429	384	366	339	301	267	237	213
	4	4.5	▪	▪	544	635	642	648	628	590	562	528	473	432	382	356	338	300	266
	4.5	5	▪	▪	▪	739	726	731	707	687	670	607	557	521	472	417	369	348	328
	5	5.5	▪	▪	▪	750	750	750	750	750	737	667	658	586	530	496	446	395	355
	5.5	6	▪	▪	▪	▪	750	750	750	750	750	750	711	633	619	558	512	470	415
	6	6.5	▪	▪	▪	▪	750	750	750	750	750	750	750	743	658	621	579	512	481
	6.5	7	▪	▪	▪	▪	▪	750	750	750	750	750	750	750	750	676	613	584	525
	7	7.5	▪	▪	▪	▪	▪	▪	750	750	750	750	750	750	750	750	686	622	593
	7.5	8	▪	▪	▪	▪	▪	▪	▪	750	750	750	750	750	750	750	750	750	690	625

Table 11. Power Matrix, in kW of Wave Dragon

Power Matrix, Wave Dragon			Period, in seconds												
			4	5	6	7	8	9	10	11	12	13	14	15	16
			5	6	7	8	9	10	11	12	13	14	15	16	17
Wave Height, in meters	0	1	160	250	360	360	360	360	360	360	320	280	250	220	180
	1	2	640	700	840	900	1,190	1,190	1,190	1,190	1,070	950	830	710	590
	2	3	▪	1,450	1,610	1,750	2,000	2,000	2,620	2,620	2,360	2,100	1,840	1,570	1,310
	3	4	▪	▪	2,840	3,220	3,710	4,200	5,320	5,320	4,430	3,930	3,440	2,950	2,460
	4	5	▪	▪	▪	4,610	5,320	6,020	7,000	7,000	6,790	6,090	5,250	3,950	3,300
	5	6	▪	▪	▪	▪	6,720	7,000	7,000	7,000	7,000	7,000	6,860	5,110	4,200
	6	7	▪	▪	▪	▪	▪	7,000	7,000	7,000	7,000	7,000	7,000	6,650	5,740

3. Results

3.1 Wind and Wave climatology from MetOceanView and PAGASA Cuyo – Station data

Using the MetOceanView Station 10 data for 2008-2018, the monthly wave climatology in Cuyo was generated (Figure 10). The monthly variability of the significant wave heights (median) ranges from 0.1 – 1.1 m with extreme significant wave heights reaching almost 2.7m (January) and outliers reaching as high as 4.1m. The outliers are usually found all throughout the year with the highest outliers in November and December. The seasonal signal of the significant wave heights related to the monsoons are also observed, wherein higher wave heights are recorded during the monsoon peaks and lower wave heights during monsoon transition period. The months with highest extreme significant wave heights and outliers coincide with the northeast monsoon months (December, January, and February).This section may be divided by subheadings. It should provide a concise and precise description of the experimental results, their interpretation, as well as the experimental conclusions that can be drawn.

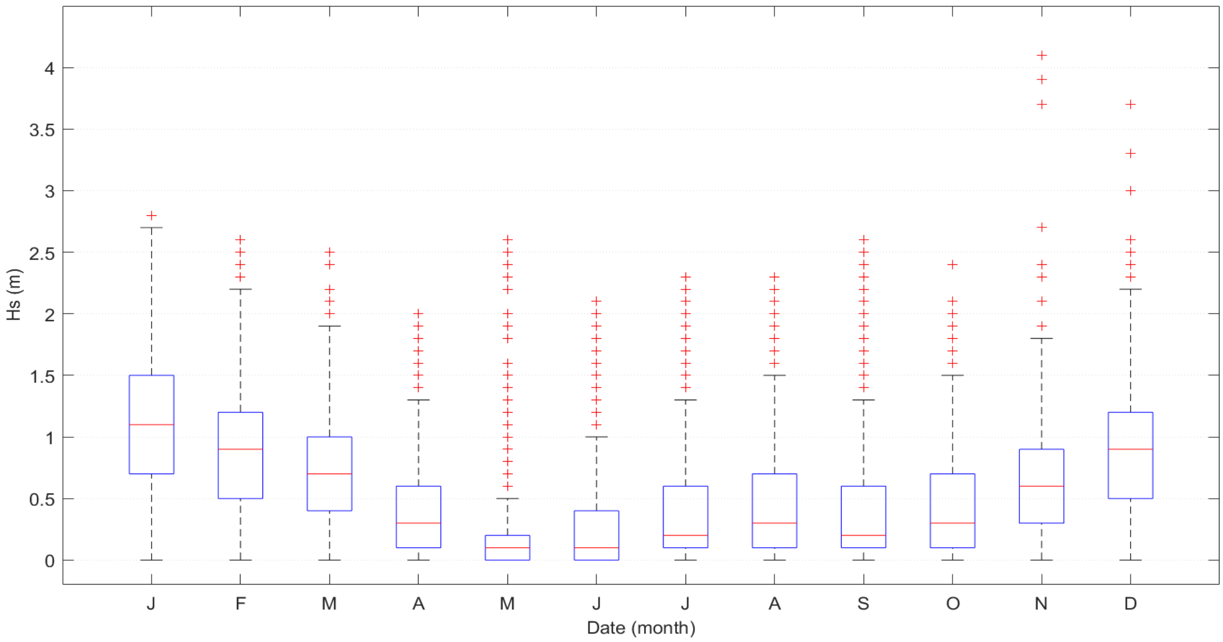

Figure 10. Box whisker plot (upper panel) and time-series plot (lower panel) of significant wave heights from MetOceanView. Red line inside the box of the box whisker plot shows the monthly median, box edges represent the 25th and 75th percentiles, the whiskers extend to the most extreme data points not considered outliers, while the red '+' marker symbol represents the outliers.

Likewise, the compass roses of significant wave height (Figure 11) and wave period (Figure 12) with propagation direction show the strong monsoonal influence with most waves clustered along the N-NNE and WSW-SW-SSW directions. It is also notable in Figure 11 that significant wave heights are higher during NE Monsoon (~25% Hs is ≥1.5m) compared to SW Monsoon (~5% Hs is ≥1.5m). This observation is also consistent with peak wave period (Figure 12), wherein ~80% (majority of the waves) is ≥4s during the NE Monsoon, while only ~40% is ≥4s during the SW monsoon.

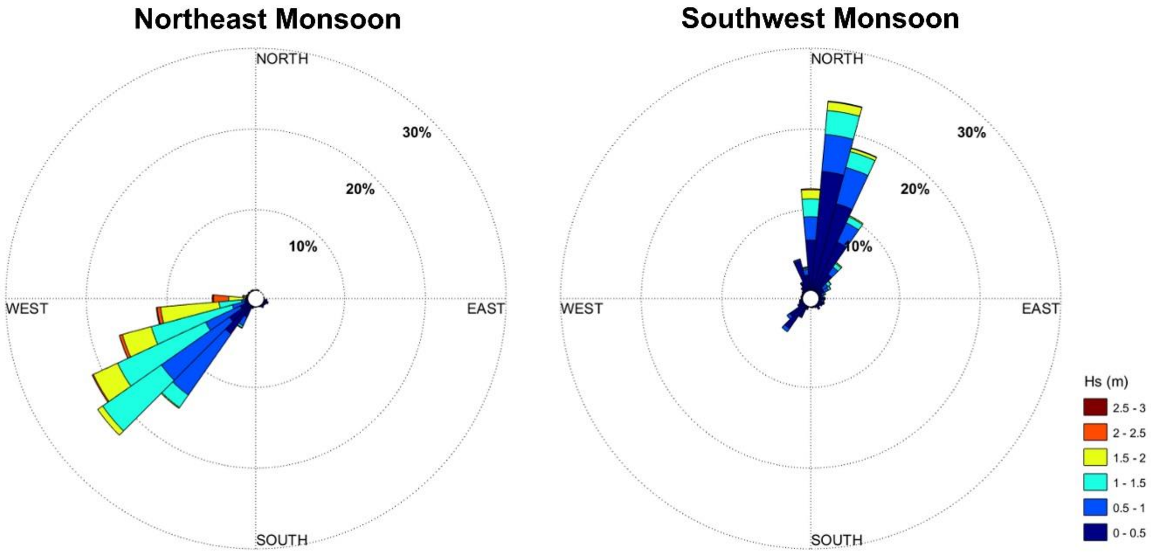

Figure 11. Compass rose of significant wave height and peak wave direction during the northeast and southwest monsoon.

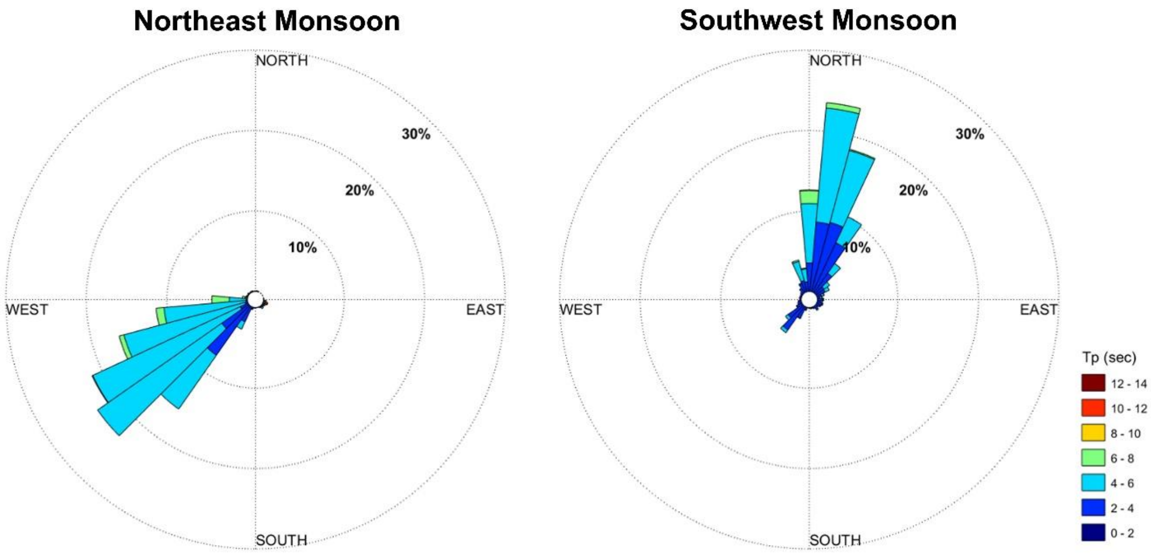

Figure 12. Compass rose of peak wave period and direction during the northeast and southwest monsoon.

In terms of wind velocities, the 2010-2018 data from MetOceanView Station 10 (3hourly data) and PAGASA wind station at Cuyo (daily data) were used to determine the wind conditions in the area. It is to be noted that the MetOceanView Station is further offshore and located ~16km north of the PAGASA Cuyo Station (more sheltered since located in land and only at 4m elevation), thus showing some differences in wind velocities (Figure 13). Noticeably, wind speeds from PAGASA station (majority below 8m/s) are weaker compared to MetOceanView data (~30% winds are ≥8m/s) (Figure 13). In terms of direction, the northeasterly wind produces stronger winds (~25% winds are ≥8m/s) compared to the southwesterly wind (~5% winds are ≥8m/s) (Figure 13). Moreover, the prominent wind direction, especially from the PAGASA Station (SSW and NE wind), agrees with the wave direction.

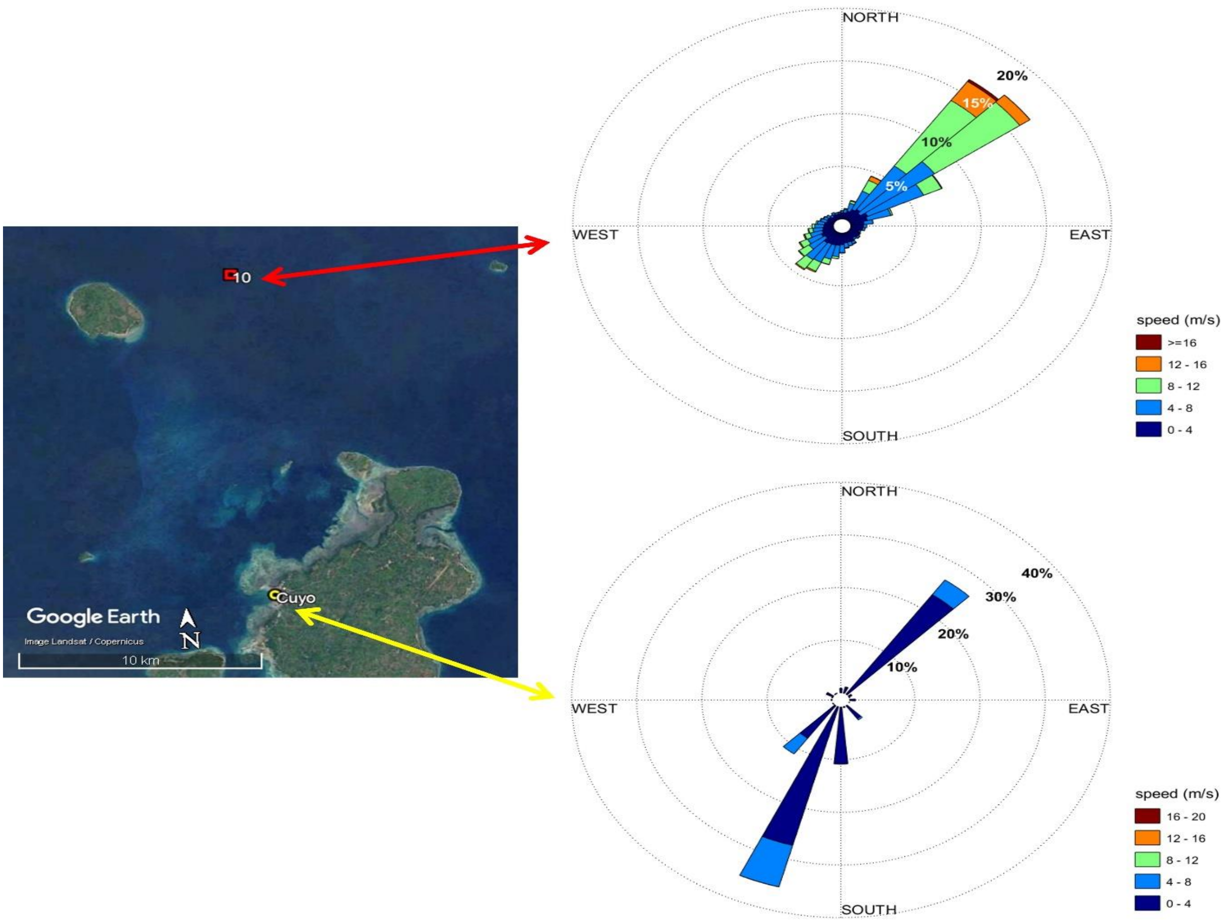

Figure 13. Wind rose of wind velocities using MetOceanView data (upper right panel) and PAGASA data (lower right panel) with the location map of both stations.

3.2 Monsoon wave model for Cuyo Island

MetOceanView's wave data and PAGASA's wind data both agrees that significant wave heights observe are related to the monsoons, wherein higher wave height are recorded and lower wave heights are during monsoon transition periods. The Wave model developed describes the wave climate surrounding the island and specifically determines the wave parameters in the six (6) points of interest which are closer to the island (Figure 14). The 6 points of interest has an average distance of 24.3 km from the island, the closest is 12.35 km (Station 1) and the farthest is 35.35 km (Station 3). During northeast monsoon season, significant wave height and peak period are highest at Station 6 (1.49 m and 4.87 s respectively), followed by Station 1 and 5, (1.43 m and 4.7 s respectively), other stations are much lower due to sheltering effects of nearby islets and the main island (Table 12) (Figure 17). Results of this points are expected to be a little lower than the MetOcean stations (Table 13) because this points are shallower [51] and more sheltered from the northeast monsoon and southwest monsoon winds [52].

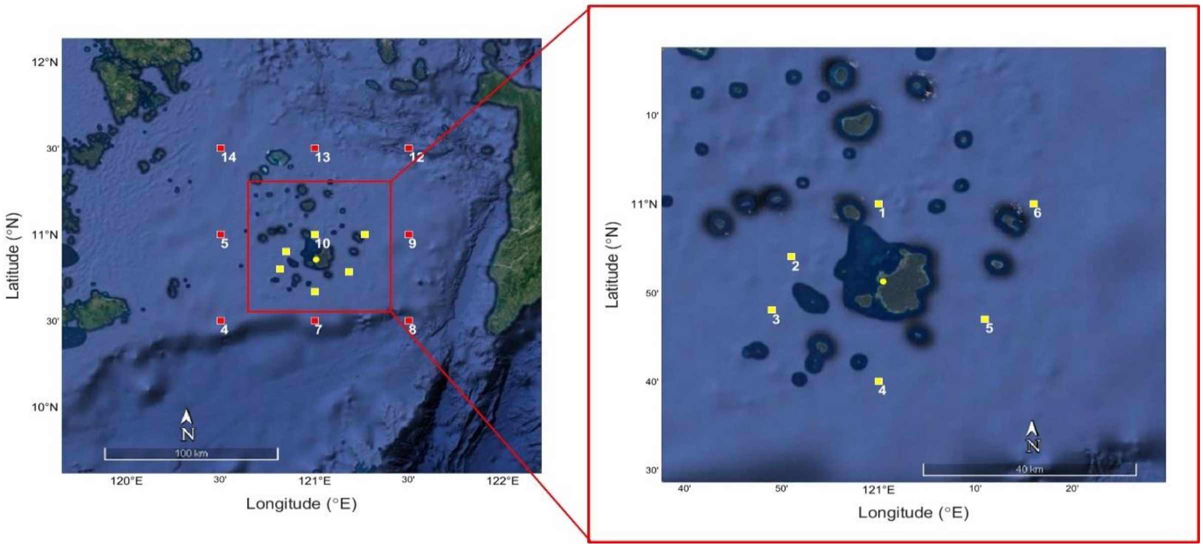

Figure 14. Location of the six (6) points of interest within the model domain

Figure 15(a) - !5(b), 16(a) - 16(b), and 17(a) – 17(b) shows the wave model result for significant wave height, peak period and energy transfer respectively during the north-east monsoon, it can be observed that in the north-eastern and south-eastern side of the island specifically on stations 1, 5 and 6 that the results are the highest having an average significant wave height (H_s), average peak period (T_P), and average wave power density (P_d) of 1.35 m, 4.79 s and 4.05 kW/m respectively, the highest at point 6 with P_d = 4.25 kW/m and T_P = 4.87 s. This results can be confirmed in Figure 17, which shows that the peak wind directions converged on these areas due to less obstructions from other islets resulting to a minimal sheltering effect and its exposure to the much stronger northeast monsoon winds, also, the water depth at those stations are much deeper compared to other stations as seen in the bathymetry data, giving a more active wave behaviour.

Table 12. Summary results of wave parameters for NE and SW Monsoon at the six (6) points of interest near the island

Station	Lon	Lat	DJF - NE Monsoon						JJA - SW Monsoon					
			Significant Wave Height (m)	Peak Period (s)	Peak Direction - U Component	Peak Direction - V Component	Total Wave Energy (J/m²)	Energy Transport (W/m)	Significant Wave Height (m)	Peak Period (s)	Peak Direction - U Componen t	Peak Direction - V Component	Total Wave Energy (J/m²)	Energy Transport (W/m)
1	121	11	1.428	4.7781	-0.5462	-1.1713	1,249.04	3,978.25	0.4258	2.5658	0.2706	0.2706	111.0763	193.8773
2	120.85	10.9	1.2547	4.361	-0.6437	-0.9193	964.3382	2,789.88	0.5449	3.0525	0.2074	0.4449	181.8621	379.0649
3	121	10.67	1.1962	4.2348	-0.4549	-0.9755	876.5134	2,361.11	0.5437	3.0582	0.281	0.4014	181.0445	366.3609
4	121.18	10.78	1.3077	4.5399	-1.0604	-0.4945	1,047.54	3,250.23	0.5657	3.1477	0.2151	0.4613	195.9928	420.4111
5	121.27	11	1.427	4.746	-0.5416	-1.1615	1,247.26	3,910.13	0.5458	3.0908	0.2072	0.4443	182.4629	388.3967
6	120.82	10.8	1.4887	4.871	-1.0977	-0.7686	1,357.53	4,246.80	0.4909	2.834	0.1145	0.4274	147.609	280.2246

Table 13. Summary results of wave parameters for NE and SW Monsoon at the nine (9) MetOcean stations

Sta	Lon	Lat	DJF - NE Monsoon						JJA - SW Monsoon					
			Significant Wave Height (m)	Peak Period (s)	Peak Direction - U Component	Peak Direction - V Component	Total Wave Energy (J/m²)	Energy Transport (W/m)	Significant Wave Height (m)	Peak Period (s)	Peak Direction - U Component	Peak Direction - V Component	Total Wave Energy (J/m²)	Energy Transport (W/m)
14	120.5	11.5	1.4042	4.7092	-1.1387	-0.531	1,207.84	3,968.37	0.5654	3.0135	0.0441	0.5046	195.8246	419.0981
13	121	11.5	1.4408	4.6642	-0.5466	-1.1721	1,271.41	3,891.82	0.5154	2.7885	0.2677	0.3823	162.6904	299.367
12	121.5	11.5	1.3	4.3625	-0.6685	-0.9547	1,035.14	2,968.29	0.5552	2.9305	0.2109	0.4524	188.8014	366.2484
5	120.5	11	1.4885	4.7751	-0.954	-0.954	1,357.16	4,280.96	0.5849	3.0785	0.0458	0.524	209.5412	431.2502
10	121	11	1.5135	4.8353	-0.7816	-1.1162	1,403.07	4,513.25	0.5274	2.8493	0.2019	0.4329	170.3466	331.3767
9	121.5	11	1.4505	4.6481	-0.748	-1.0683	1,288.67	3,923.06	0.5835	3.0309	0.2216	0.4752	208.5396	420.899
4	120.5	10.5	1.5487	4.8773	-0.9851	-0.9851	1,469.17	4,690.35	0.6025	3.1567	0.2296	0.4923	222.3052	484.0884
7	121	10.5	1.5058	4.8147	-0.7759	-1.1081	1,388.73	4,501.62	0.5889	3.0644	0.2238	0.48	212.4356	436.9373
8	121.5	10.5	1.4317	4.6555	-0.3329	-1.2423	1,255.57	3,879.12	0.5759	3.0252	0.2189	0.4693	203.1603	411.3036

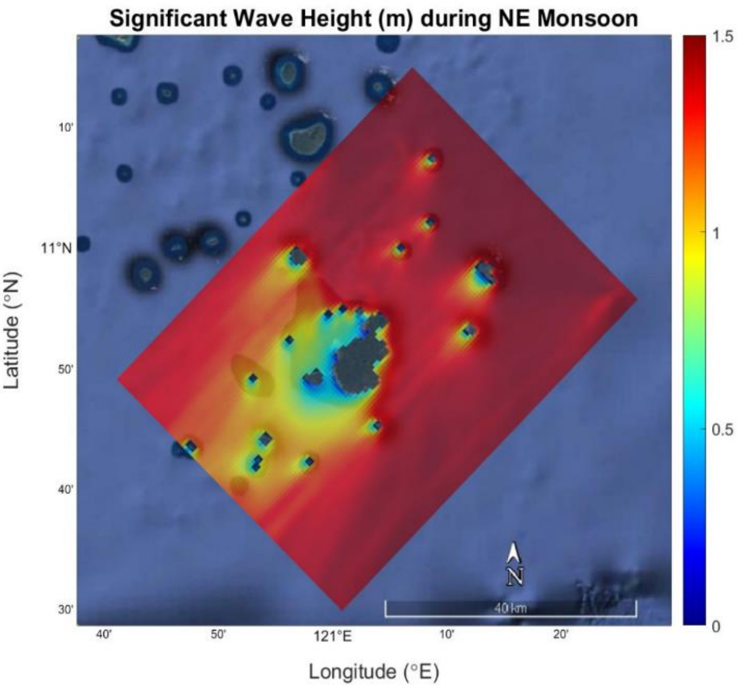

(a)

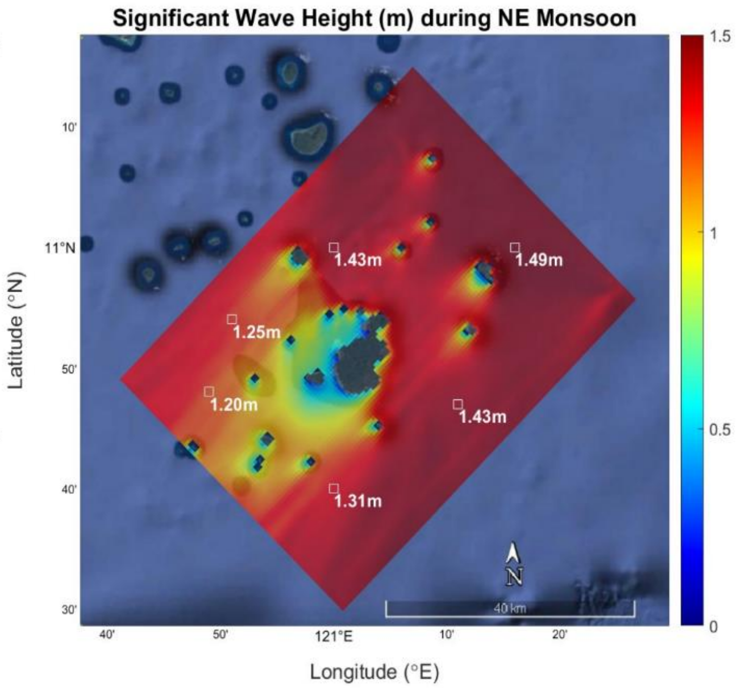

(b)

Figure 15. (a) Significant wave height (m) model during northeast monsoon season, (b) Significant wave height model indicating the average significant wave height at stations 1 – 6.

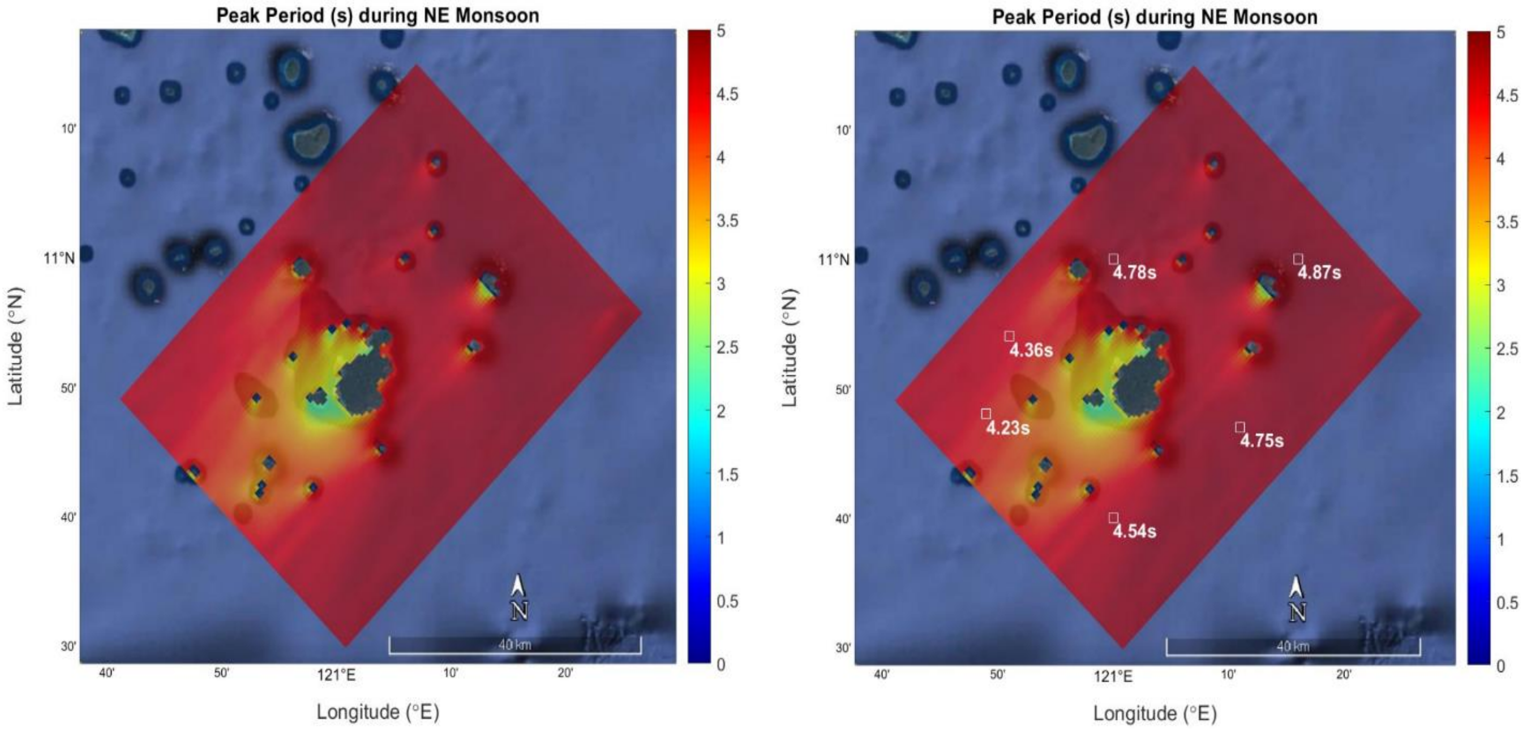

(a) **(b)**

Figure 16. (a) Peak period (s) model during northeast monsoon season, (b) Peak period model indicating the average period at stations 1 – 6.

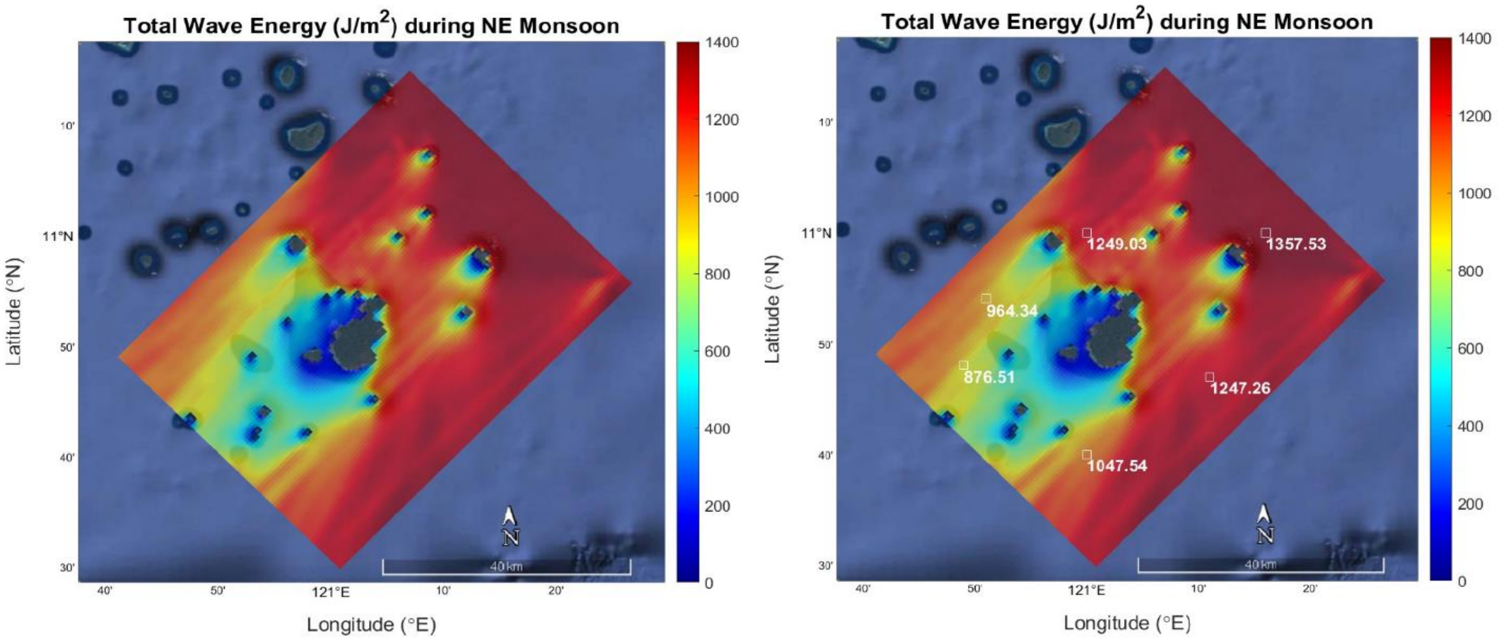

(a) **(b)**

Figure 17. (a) Wave energy propagation (J/m²) model during northeast monsoon season, (b) Wave energy propagation model, indicating the total wave energy propagated, indicating the average period at stations 1 – 6.

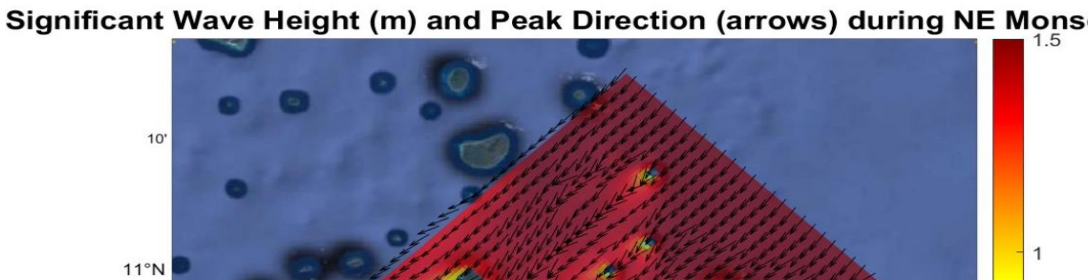

Figure 18. Significant wave height (m) and peak wind directions during northest monsoon season

Figure 19(a) – 19(b), 20(a) – 20(b), and 21(a) – 21(b) shows the wave model results for significant wave height, peak wave period and wave energy transfer model for southwest monsoon season respectively, the points 1 to 6 has an average H_s = 0.52 m, T_p = 3.37 s and P_d = 0.34 kW/m. Model results on southwest monsoon has lower values compared to the northeast monsoon model due to the sheltering effect of the main land Palawan which makes the wind passing from southwest decrease its magnitude before reaching Cuyo Island.

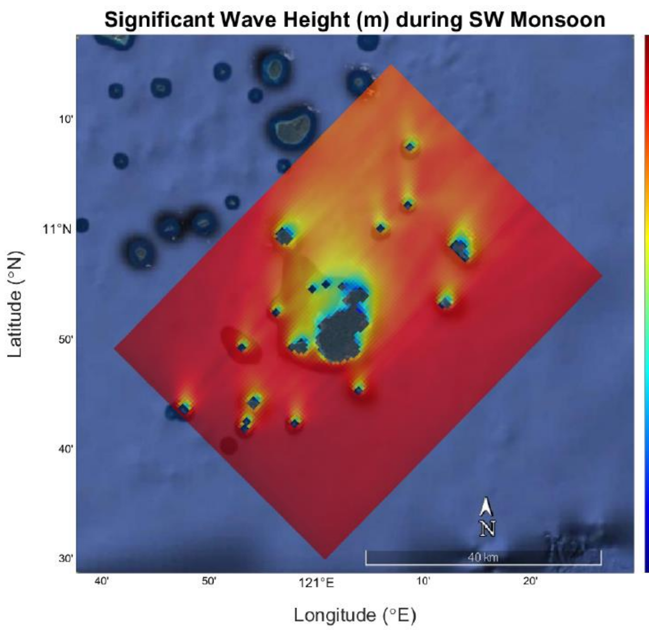

(a)

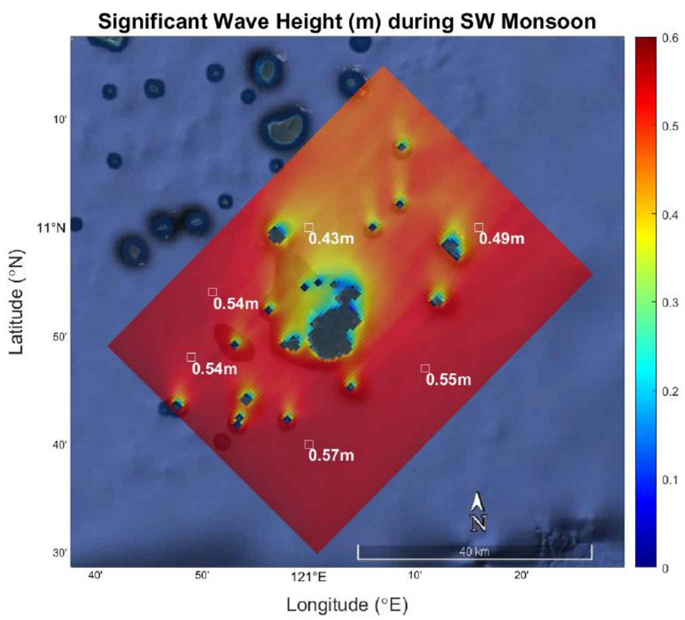

(b)

Figure 19. (a) Significant wave height (m) model during southwest monsoon season, (b) Significant wave height model indicating the average significant wave height at stations 1 – 6.

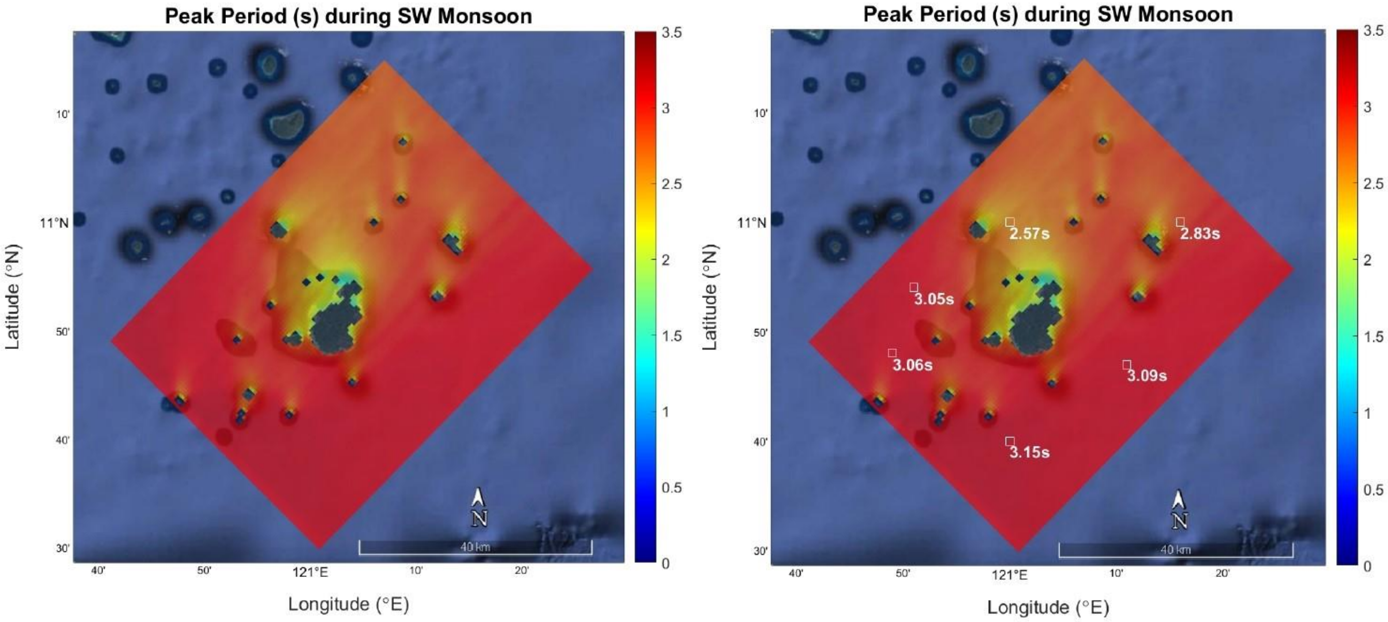

(a) (b)

Figure 20. (a) Peak period (s) model during southwest monsoon season, (b) Peak period model indicating the average peak period at stations 1 – 6.

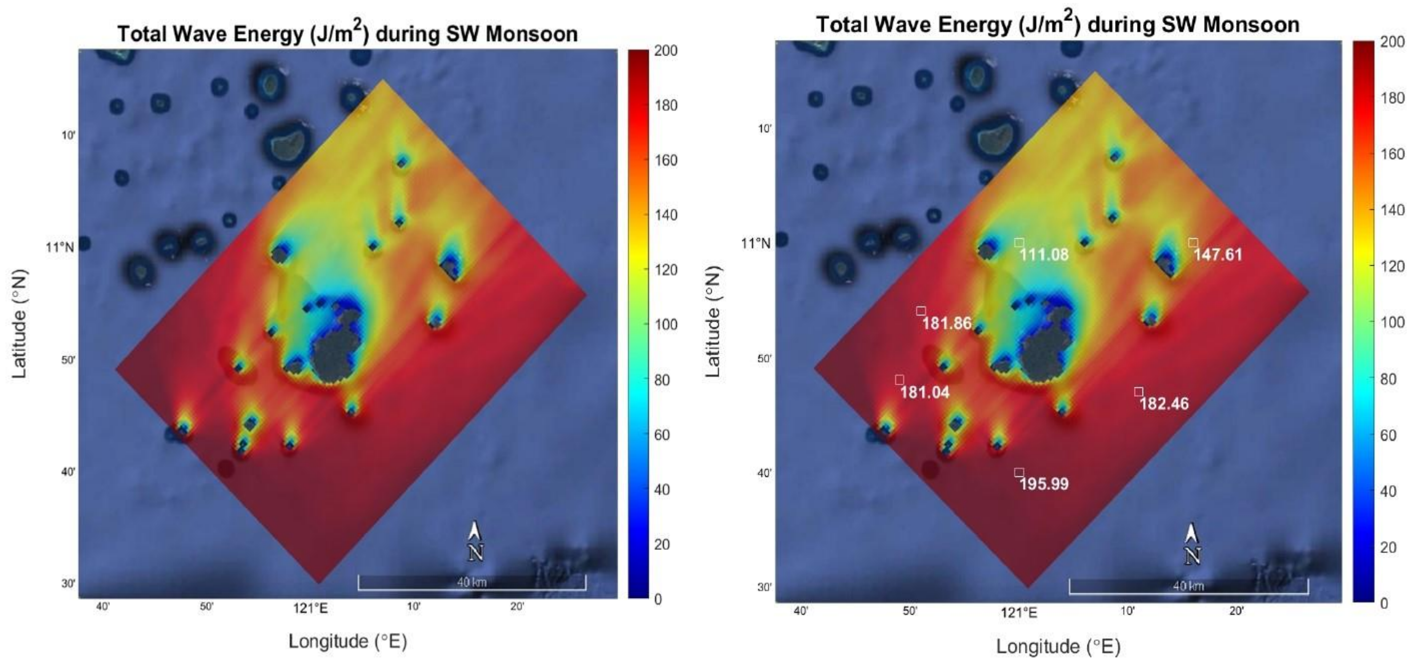

Figure 21. (a) Wave energy (J/m²) model during southwest monsoon season, (b) Wave energy model indicating the total wave energy at stations 1 – 6 duting the season.

3.3 Model validation

The resulting wave model were validated by comparing the 2018 wave hindcast produced by SWAN wave model to 2018 PAGASA - Cuyo Station's measured equivalent significant wave height. Table 14 shows the statistical metrics between the simulated and the measured parameters in all six stations, and it is shown that the simulated parameters was overestimated by the wave model compared to the measured data having an average Bias of 0.398 m, where the lowest is at station 6 at 0.38 m and the highest at station 5 at 0.42 m. A good model has an RMSE value close to zero, the closer it is the better ability of the model to accurately predict the data, here, the RMSE has an average value of 0.54, the lowest at 0.51 (Station 6) and the highest at 0.56 (Station 5), which in this case an acceptable value considering the complex topography on land where the measured wind data was taken. In general, overestimation and the degree of variance on all stations maybe explained by the following factors, the distance, location and topographical differences of the two parameters, PAGASA Cuyo Station is located on land and has an average distance from stations 1 to 6 of about 24.3 km, the nearest is 12.35 km (Station 1) and the farthest 35.35 km (Station 3). Also, the locations of Stations 1, 2 and 3 are in between small islands which may affect or distort the wind flow on the area, whereas, stations 4, 5, and 6 are more exposed with less sheltering from nearby islands (see Figure 14). Furthermore, the hub height of the equipment used to measure wind speed and wind direction in PAGASA Cuyo Station is only at 4 m where it is more prone to disturbances cause by nearby buildings and trees.

Table 14. Summary of statistical metrics between simulated and measured parameters

Station	$\bar{x}$	$\bar{y}$	Bias	RSME	SI	R
1	0.40	0.80	0.40	0.55	1.38	0.92
2	0.37	0.79	0.41	0.54	1.45	0.88
3	0.35	0.77	0.37	0.54	1.58	0.85
4	0.41	0.82	0.41	0.54	1.32	0.90
5	0.45	0.86	0.42	0.56	1.24	0.91
6	0.47	0.86	0.38	0.51	1.08	0.94

Scatter Index (SI) values also tells us a constant overestimation of the model, with all the results being higher than 1, the lowest at Station 6 at 1.08 and the highest at 1.58 (Station 3). These values may also be due to the three factors mentioned which tend to overestimate the simulated wave height. Figure 22 shows the scatter plot graph of the simulated and measured data respectively. In general, the data are clustered linearly and tend to increase exponentially at higher values starting between 0.8 to 1.0 m of the observe values. Few outliers can be observed on all stations but may not affect the overall result of the wave parameters. Finally, the data shows strong positive relationship with an average correlation coefficient (r) of 0.90, the highest is at station 6 (r = 0.94) followed by station 1 (r = 0.92) and the lowest at station 3 (r = 0.85) (Figure 23).

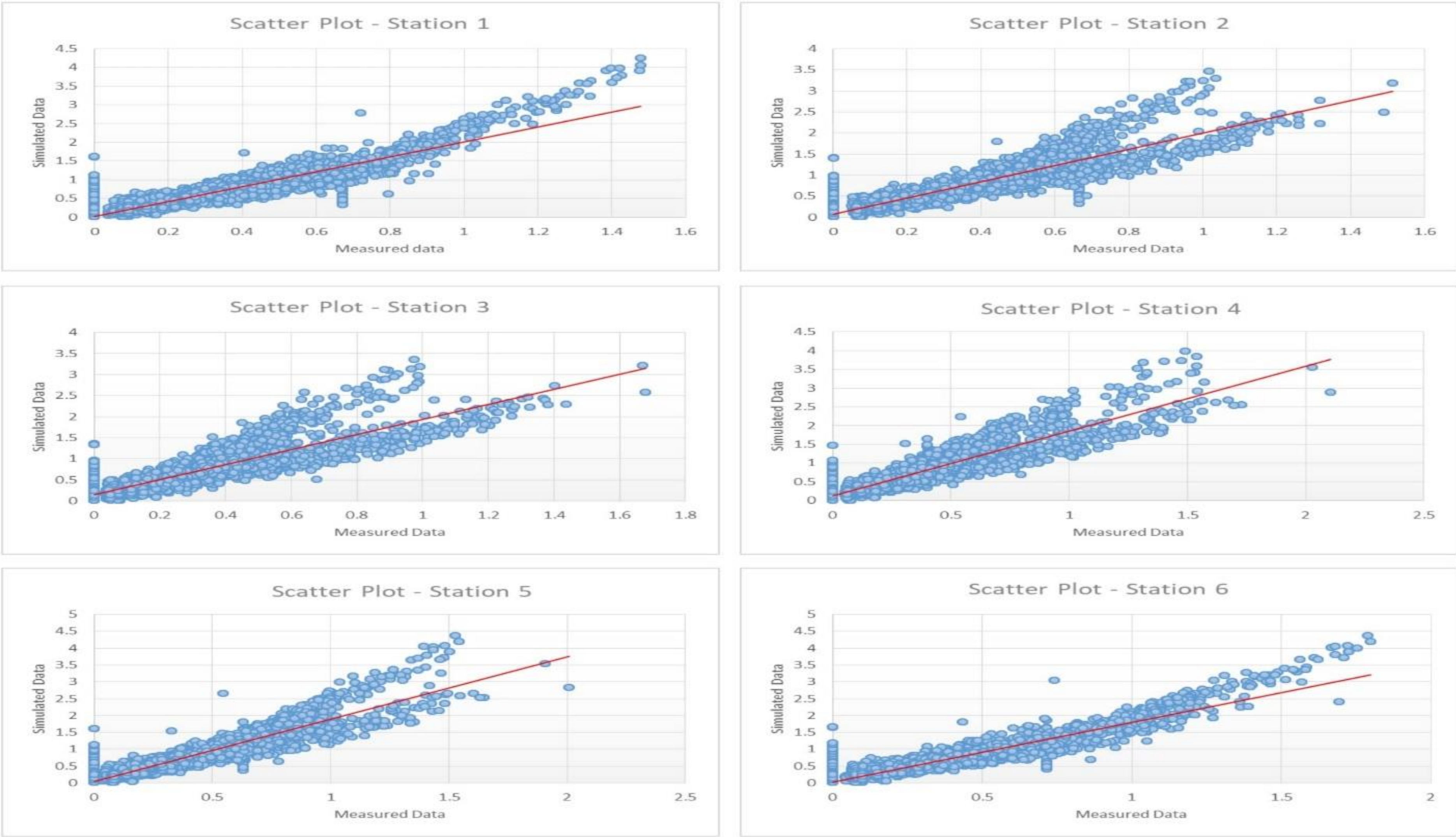

Figure 22. Scatter Plot Graph of Stations 1 – 6

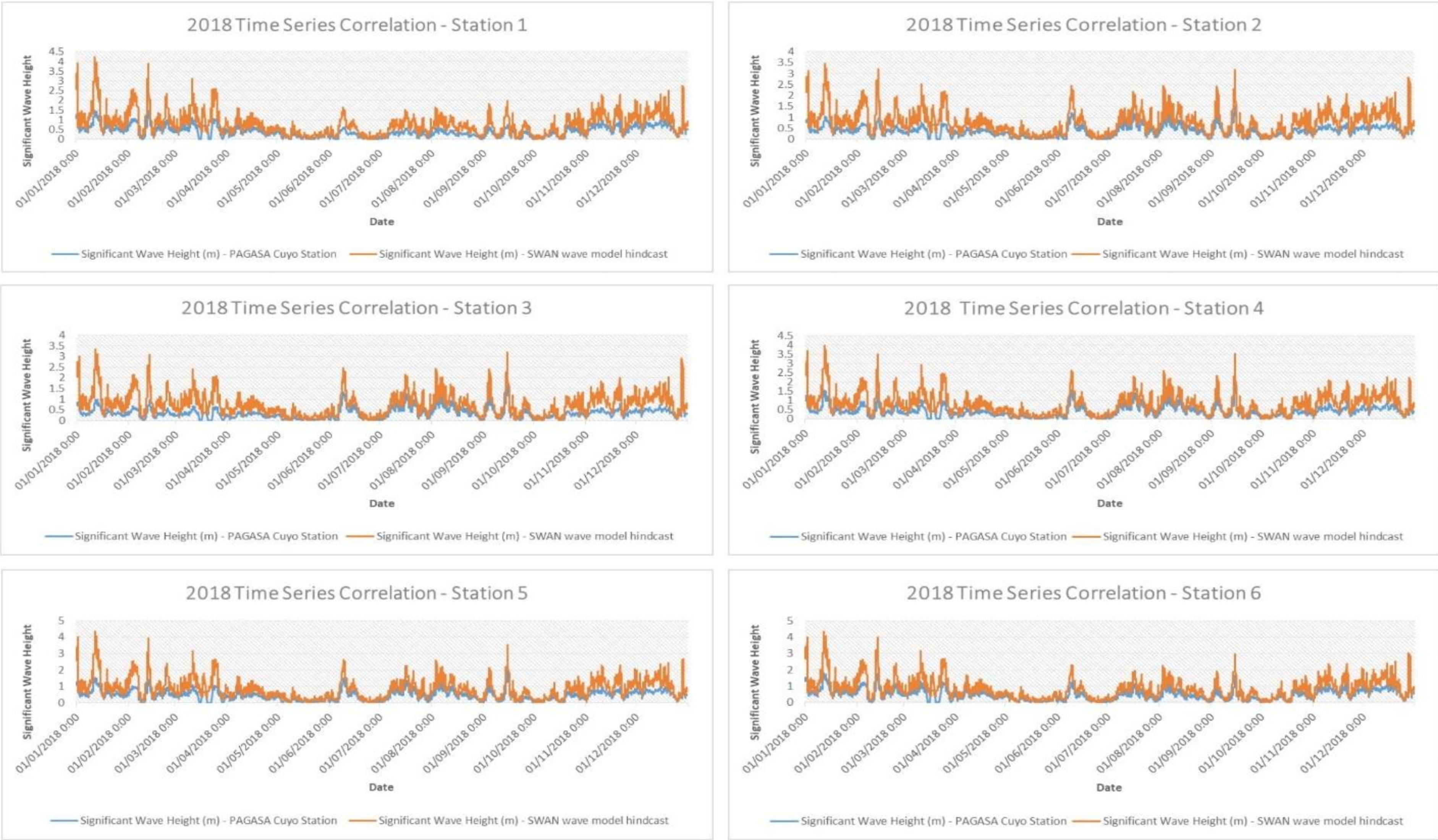

Figure 24. 2018 Time Series Correlation between the simulated and measured data at Stations 1 - 6

3.4 Annual Energy production (AEP)

Table 15 shows the annual energy production of the three wave energy converters computed using Equation 8. Station 5 and 6 draws the highest energy production on all WEC's tested, $AEP_{WaveBouy}$ = 43.761 MWh and 43.617 MWh, $AEP_{Pelamis}$ = 216.786 MWh and 213.816 MWh and $AEP_{Wave\ Dragon}$ = 2462.66 MWh and 2427 MWh respectively. Capacity factors for three WEC's are <8%, this is because most of the data are at lower values and are not within the devices energy production capability. A sample computation is presented in Table 16 – 18, and the rest of the computations can be seen in Appendix A.

Table 15. Annual energy production of the three wave energy converters, in MWh

Wave Energy Converter	Annual Energy Production (AEP), in MWh					
	Station 1	Station 2	Station 3	Station 4	Station 5	Station 6
WaveBouy	33.681	23.526	19.826	33.954	43.761	43.617
Pelamis	173.421	127.314	109.149	176.746	216.786	213.816
Wave Dragon	2046.15	1805.07	1657.62	2174.61	2462.04	2427.66

Table 16. Sample computation of the AEP for AquaBouy at Station 4

AquaBouy Annual Energy Production							
Station 4		Period (Tp), in seconds					
		5	6	7	8	9	10
		6	7	8	9	10	11
Wave Height (Hs), in meters: 0	0.5	▪	0.024	0.036	0.03	▪	0.024
0.5	1	▪	▪	▪	▪	▪	▪
1	1.5	0.078	▪	▪	▪	▪	▪
1.5	2	11.016	▪	▪	▪	▪	▪
2	2.5	8.769	1.41	▪	▪	▪	▪
2.5	3	▪	6.936	▪	▪	▪	▪
3	3.5	▪	3.069	▪	▪	▪	▪
3.5	4	▪	▪	2.562	▪	▪	▪
Annual Energy Production = 33.954 MWh							

Table 17. Sample computation of AEP for Pelamis at Station 1

Pelamis Annual Energy Production								
Station 1		Period (Tp), in seconds						
		4.5	5	5.5	6	6.5	7	7.5
		5	5.5	6	6.5	7	7.5	8
Wave Height (Hs), in meters: 0	0.5	▪	▪	▪	▪	▪	▪	▪
0.5	1	▪	▪	▪	▪	▪	▪	▪
1	1.5	14.496	▪	▪	▪	▪	▪	▪
1.5	2	12.141	30.888	3.795	▪	▪	▪	▪
2	2.5	▪	0.414	36.72	5.724	▪	▪	▪
2.5	3	▪	▪	▪	24.705	1.992	▪	▪
3	3.5	▪	▪	▪	▪	22.338	▪	▪
3.5	4	▪	▪	▪	▪	▪	16.38	▪
4	4.5	▪	▪	▪	▪	▪	1.944	1.884
Annual Energy Production = 173.421 MWh								

Table 18. Sample computation of AEP for Wave Dragon at Station 6

Wave Dragon Annual Energy Production								
Station 6		Period (Tp), in seconds						
		4	5	6	7	8	9	10
		5	6	7	8	9	10	11
Wave Height (Hs), in meters: 0	1	21.12	1.68	1.08	1.08	▪	1.08	1.08
1	2	1094.4	396.9	▪	▪	▪	▪	▪
2	3	▪	365.4	236.67	▪	▪	▪	▪
3	4	▪	▪	170.4	67.62	▪	▪	▪
4	5	▪	▪	▪	69.15	▪	▪	▪
Annual Energy Production = 2427.66 MWh								

4.0 Conclusions

Wave energy resource assessment in the Philippines ranges from 10 – 20 kW/m as reported in Quitoras et. al [9], in the 47 sites under the coastal regions of Catanduanes, Samar, Siargao Island, Surigao del Sur and Western Luzon. In Wan et. al, [53] along Luzon strait, exploitable wave energy resource is at 10 – 15 kW/m, to which, agrees with the findings in [9]. In Dumaran study [8], the wave energy resource surrounding the island within 100 km radius is less than 4.5 kW/m, this is in agreement with Mirzae et. al [54] where semi-enclosed sea or sheltered areas has a lower probability of harnessing wave energy resource that will exceed 5 kW/m at any season. With the same topographical characteristic as Dumaran Island, resulting nearshore P_d in Cuyo Island during monsoon seasons is also less than 5 kW/m, the highest at 4.25 kW/m (Station 6) and lowest at 2.36 kW/m (Station 3) during northeast monsoon (Amihan Season) and during southeast monsoon the highest and lowest P_d is at 0.42 kW/m and 0.19 kW/m respectively. Although the simulated results tends to overestimate the significant wave height as compared with the equivalent significant wave height of the measured wind speed on site with average

Bias, RSME and SI values of 0.398, 0.54, and 1.34 respectively, the simulated and measured data has a strong positive relationship with an average correlation coefficient (r) of 0.90, the highest at 0.94 (Station 6) and the lowest at 0.85 (Station 3). This signifies that as a whole, the measured wind data is in agreement with the simulated wave data, and therefore, can be used as reference in analysing the nearshore wave energy resource surrounding the island of Cuyo either for exploitation or testing of nearshore wave energy converter [55, 56]. The AEP is highest at Station 5 for all WEC's tested with Wave Dragon having $AEP_{Wave\ Dragon}$ = 2,462.04 MWh with a capacity factor of 7%, this happens because the majority of the data falls on lower values of H_s and T_p where the wave energy device is not capable of producing energy. At the moment, the minimum wave energy resource for wave farm development is 5 kW/m globally, but with the speeding development of wave energy converters, and the need for electrifying isolated small island community in a semi-enclosed sea, development may soon be shifted for milder wave energy resource lower than 5 kW/m.

To predict more accurately and enhanced the high resolution wave model of the wave energy resource in an isolated island of the same characteristics, it is recommended to have an on-site measurement of the wave parameters for a minimum of 1 year or maybe longer.

Author Contributions: Conceptualization, J.P. and M.A.; methodology, J.P. and M.A.; software, J.P.; validation, J.P., formal analysis, J.P. and M.A.; investigation, J.P.; resources, J.P.; data curation, J.P.; writing—original draft preparation, J.P.; writing—review and editing, J.P. and M.A.; visualization, J.P. and M.A.; supervision, revision and verifying the results J.P. and M.A. The authors have read and agreed to the published version of the manuscript.

Funding: The scientific work was supported by the Department of Science and Technology – Engineering Research and Development for Technology (DOST – ERDT), Republic of the Philippines.

Acknowledgments: The authors would like to thank the University of San Carlos DOST –Engineering Research and Development for Technology (ERDT) Scholarship, Center for Research and Energy Systems Technology (CREST) and Palawan State University for their support and motivations in conducting this research. To the support of the following individuals, Dr. Severin Thiebut, Senior Physical Oceanographer, MetOcean for allowing us to use the 40-year hindcast data. To Ms. Shalou Maratas of PAGASA – Climate and Agrometeorological Data section (CADS) for the 9-year on-site wind parameters data and lastly, to Engr. Weslie Capute and Ms. Princess Hope Bilgera of Oceanpixel, Pte. Ltd, Singapore for supporting this research work.

Conflicts of Interest: The authors declare no conflict of interest.

Appendix A

Computations of the Annual Energy Production (AEP) on stations 1 – 6 for the three wave energy devices.

1. WaveBouy

Table A1. AEP at Station 1

AquaBouy Annual Energy Production								
Station 1			Period (Tp), in seconds					
			5	6	7	8	9	10
			6	7	8	9	10	11
Wave Height (Hs), in meters	0	0.5	▪	▪	0.033	0.033	0.03	0.024
	0.5	1	▪	▪	▪	▪	▪	▪
	1	1.5	▪	▪	▪	▪	▪	▪
	1.5	2	9.216	▪	▪	▪	▪	▪
	2	2.5	7.659	1.269	▪	▪	▪	▪
	2.5	3	▪	5.916	▪	▪	▪	▪
	3	3.5	▪	4.743	▪	▪	▪	▪
	3.5	4	▪	▪	4.05	▪	▪	▪
	4	4.5	▪	▪	0.732	▪	▪	▪
Annual Energy Production = 33.681 MWh								

Table A2. AEP at Station 2

AquaBouy Annual Energy Production								
Station 2			Period (Tp), in seconds					
			5	6	7	8	9	10
			6	7	8	9	10	11
Wave Height (Hs), in meters	0	0.5	▪	▪	0.033	0.033	0.024	0.024
	0.5	1	▪	▪	▪	▪	▪	▪
	1	1.5	▪	▪	▪	▪	▪	▪
	1.5	2	7.56	▪	▪	▪	▪	▪
	2	2.5	8.325	0.564	▪	▪	▪	▪
	2.5	3	1.62	2.856	▪	▪	▪	▪
	3	3.5	▪	2.511	▪	▪	▪	▪
	3.5	4	▪	▪	2.562	▪	▪	▪
Annual Energy Production = 23.526 MWh								

Table A3. AEP at Station 3

AquaBouy Annual Energy Production								
Station 3			Period (Tp), in seconds					
			5	6	7	8	9	10
			6	7	8	9	10	11
Wave Height (Hs), in meters	0	0.5	▪	0.024	0.036	0.03	0.024	▪
	0.5	1	▪	▪	▪	▪	▪	▪
	1	1.5	▪	▪	▪	▪	▪	▪
	1.5	2	6.624	▪	▪	▪	▪	▪
	2	2.5	6.882	0.705	▪	▪	▪	▪
	2.5	3	1.296	2.244	▪	▪	▪	▪
	3	3.5	▪	1.953	▪	▪	▪	▪
Annual Energy Production = 19.818 MWh								

Table A4. AEP at Station 4

AquaBouy Annual Energy Production							
Station 4		Period (Tp), in seconds					
		5	6	7	8	9	10
		6	7	8	9	10	11
Wave Height (Hs), in meters							
0	0.5	▪	0.024	0.036	0.03	▪	0.024
0.5	1	▪	▪	▪	▪	▪	▪
1	1.5	0.078	▪	▪	▪	▪	▪
1.5	2	11.016	▪	▪	▪	▪	▪
2	2.5	8.769	1.41	▪	▪	▪	▪
2.5	3	▪	6.936	▪	▪	▪	▪
3	3.5	▪	3.069	▪	▪	▪	▪
3.5	4	▪	▪	2.562	▪	▪	▪
Annual Energy Production = 33.954 MWh							

Table A5. AEP at Station 5

AquaBouy Annual Energy Production							
Station 5		Period (Tp), in seconds					
		5	6	7	8	9	10
		6	7	8	9	10	11
Wave Height (Hs), in meters							
0	0.5	▪	0.024	0.036	▪	0.024	0.024
0.5	1	▪	▪	▪	▪	▪	▪
1	1.5	▪	▪	▪	▪	▪	▪
1.5	2	12.744	▪	▪	▪	▪	▪
2	2.5	9.546	1.974	▪	▪	▪	▪
2.5	3	▪	8.364	▪	▪	▪	▪
3	3.5	▪	4.743	▪	▪	▪	▪
3.5	4	▪	▪	2.928	▪	▪	▪
4	4.5	▪	▪	3.345	▪	▪	▪
Annual Energy Production = 43.761 MWh							

Table A6. AEP at Station 6

AquaBouy Annual Energy Production							
Station 6		Period (Tp), in seconds					
		5	6	7	8	9	10
		6	7	8	9	10	11
Wave Height (Hs), in meters							
0	0.5	▪	0.024	0.036	▪	0.024	0.024
0.5	1	▪	▪	▪	▪	▪	▪
1	1.5	0.039	▪	▪	▪	▪	▪
1.5	2	13.536	▪	▪	▪	▪	▪
2	2.5	9.324	1.974	▪	▪	▪	▪
2.5	3	▪	7.14	▪	▪	▪	▪
3	3.5	▪	5.58	▪	▪	▪	▪
3.5	4	▪	▪	2.562	▪	▪	▪
4	4.5	▪	▪	3.345	▪	▪	▪
Annual Energy Production = 43.617 MWh							

2. Pelamis

Table A7. AEP at Station 1

Pelamis Annual Energy Production									
Station 1			Period (Tp), in seconds						
			4.5	5	5.5	6	6.5	7	7.5
			5	5.5	6	6.5	7	7.5	8
Wave Height (Hs), in meters	0	0.5	▪	▪	▪	▪	▪	▪	▪
	0.5	1	▪	▪	▪	▪	▪	▪	▪
	1	1.5	14.496	▪	▪	▪	▪	▪	▪
	1.5	2	12.141	30.888	3.795	▪	▪	▪	▪
	2	2.5	▪	0.414	36.72	5.724	▪	▪	▪
	2.5	3	▪	▪	▪	24.705	1.992	▪	▪
	3	3.5	▪	▪	▪	▪	22.338	▪	▪
	3.5	4	▪	▪	▪	▪	▪	16.38	▪
	4	4.5	▪	▪	▪	▪	▪	1.944	1.884
Annual Energy Production = 173.431 MWh									

Table A8. AEP at Station 2

Pelamis Annual Energy Production									
Station 2			Period (Tp), in seconds						
			4.5	5	5.5	6	6.5	7	7.5
			5	5.5	6	6.5	7	7.5	8
Wave Height (Hs), in meters	0	0.5	▪	▪	▪	▪	▪	▪	▪
	0.5	1	▪	▪	▪	▪	▪	▪	▪
	1	1.5	12	▪	▪	▪	▪	▪	▪
	1.5	2	15.561	27.192	0.69	▪	▪	▪	▪
	2	2.5	▪	11.178	25.92	2.544	▪	▪	▪
	2.5	3	▪	▪	7.8	12.81	▪	▪	▪
	3	3.5	▪	▪	▪	3.735	7.884	▪	▪
	3.5	4	▪	▪	▪	▪	▪	▪	▪
	4	4.5	▪	▪	▪	▪	▪	▪	▪
Annual Energy Production = 127.314 MWh									

Table A9. AEP at Station 3

Pelamis Annual Energy Production									
Station 3			Period (Tp), in seconds						
			4.5	5	5.5	6	6.5	7	7.5
			5	5.5	6	6.5	7	7.5	8
Wave Height (Hs), in meters	0	0.5	▪	▪	▪	▪	▪	▪	▪
	0.5	1	▪	▪	▪	▪	▪	▪	▪
	1	1.5	9.12	▪	▪	▪	▪	▪	▪
	1.5	2	16.416	22.968	1.725	▪	▪	▪	▪
	2	2.5	▪	9.522	21.06	3.18	▪	▪	▪
	2.5	3	▪	▪	6.24	10.065	▪	▪	▪
	3	3.5	▪	▪	▪	6.225	2.628	▪	▪
	3.5	4	▪	▪	▪	▪	▪	▪	▪
	4	4.5	▪	▪	▪	▪	▪	▪	▪
Annual Energy Production = 109.149 MWh									

Table A10. AEP at Station 4

Pelamis Annual Energy Production									
Station 4			Period (Tp), in seconds						
			4.5	5	5.5	6	6.5	7	7.5
			5	5.5	6	6.5	7	7.5	8
Wave Height (Hs), in meters	0	0.5	▪	▪	▪	▪	▪	▪	▪
	0.5	1	▪	▪	▪	▪	▪	▪	▪
	1	1.5	17.088	0.3	▪	▪	▪	▪	▪
	1.5	2	10.944	38.016	3.105	▪	▪	▪	▪
	2	2.5	▪	2.07	39.96	6.36	▪	▪	▪
	2.5	3	▪	▪	▪	27.45	3.984	▪	▪
	3	3.5	▪	▪	▪	1.245	13.14	▪	▪
	3.5	4	▪	▪	▪	▪	1.62	11.47	▪
	4	4.5	▪	▪	▪	▪	▪	▪	▪
Annual Energy Production = 176.748 MWh									

Table A11. AEP at Station 5

Pelamis Annual Energy Production									
Station 5			Period (Tp), in seconds						
			4.5	5	5.5	6	6.5	7	7.5
			5	5.5	6	6.5	7	7.5	8
Wave Height (Hs), in meters	0	0.5	▪	▪	▪	▪	▪	▪	▪
	0.5	1	▪	▪	▪	▪	▪	▪	▪
	1	1.5	18.432	▪	▪	▪	▪	▪	▪
	1.5	2	12.312	43.032	4.83	▪	▪	▪	▪
	2	2.5	▪	0.414	45.9	8.904	▪	▪	▪
	2.5	3	▪	▪	▪	32.94	4.98	▪	▪
	3	3.5	▪	▪	▪	▪	22.338	▪	▪
	3.5	4	▪	▪	▪	▪	▪	13.1	▪
	4	4.5	▪	▪	▪	▪	▪	5.832	3.768
Annual Energy Production = 216.786 MWh									

Table A12. AEP at Station 6

Pelamis Annual Energy Production									
Station 6			Period (Tp), in seconds						
			4.5	5	5.5	6	6.5	7	7.5
			5	5.5	6	6.5	7	7.5	8
Wave Height (Hs), in meters	0	0.5	▪	▪	▪	▪	▪	▪	▪
	0.5	1	▪	▪	▪	▪	▪	▪	▪
	1	1.5	19.296	0.15	▪	▪	▪	▪	▪
	1.5	2	9.405	45.672	5.175	▪	▪	▪	▪
	2	2.5	▪	▪	45.36	8.904	▪	▪	▪
	2.5	3	▪	▪	▪	26.535	5.976	▪	▪
	3	3.5	▪	▪	▪	▪	26.28	▪	▪
	3.5	4	▪	▪	▪	▪	▪	11.47	▪
	4	4.5	▪	▪	▪	▪	▪	5.832	3.768
Annual Energy Production = 213.819MWh									

3. Wave Dragon

Table A13. AEP at Station 1

Wave Dragon Annual Energy Production

Station 1		Period (Tp), in seconds							
		4	5	6	7	8	9	10	11
Wave Height (Hs), in meters		5	6	7	8	9	10	11	12
0	1	4.8	0.84	▪	1.08	▪	1.08	1.08	▪
1	2	1015.7	268.8	▪	▪	▪	▪	▪	▪
2	3	▪	300.15	183.54	▪	▪	▪	▪	▪
3	4	▪	▪	144.84	96.6	▪	▪	▪	▪
4	5	▪	▪	▪	27.66	▪	▪	▪	▪

Annual Energy Production = 2046.15 MWh

Table A14. AEP at Station 2

Wave Dragon Annual Energy Production

Station 2		Period (Tp), in seconds							
		4	5	6	7	8	9	10	11
Wave Height (Hs), in meters		5	6	7	8	9	10	11	12
0	1	12.48	2.52	▪	1.08	▪	▪	1.08	1.08
1	2	1033	220.5	▪	▪	▪	▪	▪	▪
2	3	▪	369.75	86.94	▪	▪	▪	▪	▪
3	4	▪	▪	76.68	▪	▪	▪	▪	▪
4	5	▪	▪	▪	69.15	▪	▪	▪	▪

Annual Energy Production = 1805.07 MWh

Table A15. AEP at Station 3

Wave Dragon Annual Energy Production

Station 3		Period (Tp), in seconds							
		4	5	6	7	8	9	10	11
Wave Height (Hs), in meters		5	6	7	8	9	10	11	12
0	1	12	2.52	1.08	1.08	▪	1.08	1.08	▪
1	2	1004.2	193.2	▪	▪	▪	▪	▪	▪
2	3	▪	304.5	77.28	▪	▪	▪	▪	▪
3	4	▪	▪	59.64	▪	▪	▪	▪	▪
4	5	▪	▪	▪	▪	▪	▪	▪	▪

Annual Energy Production = 1657.62 MWh

Table A16. AEP at Station 4

Wave Dragon Annual Energy Production

Station 4		Period (Tp), in seconds							
		4	5	6	7	8	9	10	11
Wave Height (Hs), in meters		5	6	7	8	9	10	11	12
0	1	17.28	2.52	1.08	1.08	▪	1.08	1.08	▪
1	2	1090.6	333.9	▪	▪	▪	▪	▪	▪
2	3	▪	343.65	212.52	▪	▪	▪	▪	▪
3	4	▪	▪	102.24	67.62	▪	▪	▪	▪
4	5	▪	▪	▪	▪	▪	▪	▪	▪

Annual Energy Production = 2174.61 MWh

Table A17. AEP at Station 5

Wave Dragon Annual Energy Production										
Station 5			Period (Tp), in seconds							
			4	5	6	7	8	9	10	11
			5	6	7	8	9	10	11	12
Wave Height (Hs), in meters	0	1	15.84	2.52	1.08	1.08	▪	1.08	1.08	▪
	1	2	1136.6	371.7	▪	▪	▪	▪	▪	▪
	2	3	▪	374.1	265.65	▪	▪	▪	▪	▪
	3	4	▪	▪	144.84	77.28	▪	▪	▪	▪
	4	5	▪	▪	▪	69.15	▪	▪	▪	▪
Annual Energy Production = 2462.04 MWh										

Table A18. AEP at Station 6

Wave Dragon Annual Energy Production										
Station 6			Period (Tp), in seconds							
			4	5	6	7	8	9	10	11
			5	6	7	8	9	10	11	12
Wave Height (Hs), in meters	0	1	21.12	1.68	1.08	1.08	▪	1.08	1.08	▪
	1	2	1094.4	396.9	▪	▪	▪	▪	▪	▪
	2	3	▪	365.4	236.67	▪	▪	▪	▪	▪
	3	4	▪	▪	170.4	67.62	▪	▪	▪	▪
	4	5	▪	▪	▪	69.15	▪	▪	▪	▪
Annual Energy Production = 2427.66 MWh										

References

1. IRENA (2017): Renewables Readiness Assessment, International Renewable Energy Agency, Abu Dhabi. Available online: https://www.irena.org/publications/2017/Mar/Renewables-Readiness-Assessment-The-Philippines, (Accessed on 20 May, 2022)
2. 2018 Power Supply and Demand Highlights, Republic of the Philippines, Department of Energy, EPIMB. Available online: http://161.49.106.166/electric-power/2018-power-supply-and-demand-highlights, (Accessed on 20 May, 2022)
3. Philippine Energy Plan 2017 – 2040: Sectoral Plans and Roadmaps, Department of Energy. Available online: https://www.doe.gov.ph/pep/renewable-energy-roadmap-2017-2040?withshield=1 (Accessed 20 May, 2022)
4. Veigas, M., Ramos, V., & Iglesias, G. (2014). A wave farm for an island: Detailed effects on the nearshore wave climate. *Energy*, *69*, 801-812. https://doi.org/10.1016/j.energy.2014.03.076
5. Rusu, E., & Onea, F. (2019). An assessment of the wind and wave power potential in the island environment. *Energy*, *175*, 830-846., https://doi.org/10.1016/j.energy.2019.03.130
6. Gonçalves, M., Martinho, P., & Soares, C. G. (2014). Assessment of wave energy in the Canary Islands. *Renewable Energy*, *68*, 774-784., https://doi.org/10.1016/j.renene.2014.03.017
7. Moschos, E., Manou, G., Dimitriadis, P., Afentoulis, V., Koutsoyiannis, D., & Tsoukala, V. K. (2017). Harnessing wind and wave resources for a Hybrid Renewable Energy System in remote islands: a combined stochastic and deterministic approach. *Energy Procedia*, *125*, 415-424., https://doi.org/10.1016/j.egypro.2017.08.084
8. Aminudin, A., Teh, H. M., & Pacaldo, J. (2021). Wave Energy Assessment in Dumaran Island, Palawan, Philippines. *International Journal of Coastal and Offshore Engineering*, *6*(5), 51-63. Available online: https://www.ijcoe.org/article_152614_2defe337bb73a06acf5d3e6a8b118777.pdf
9. Quitoras, Marvin & Abundo, Michael & Danao, Louis. (2018). A techno-economic assessment of wave energy resources in the Philippines. Renewable and Sustainable Energy Reviews. 88. 68-81., https://doi.org/10.1016/j.rser.2018.02.016
10. Asian Development Bank. Wave Energy Conversion and Ocean Thermal Energy Conversion Potential in Developing Member Countries. Available online: https://www.adb.org/publications/wave-energy-conversion-and-ocean-thermal-energy-conversionpotential-developing-member (Accessed on 20 May, 2022)
11. Cornett AM. A global wave energy resource assessment. Vancouver, Canada: International Offshore and Polar Engineering Conference; 2008. p. 1–9.
12. Mork G, Barstow S, Kabuth A, Pontes Meresa. Assessing the global wave energy potential, Shanghai, China. In: Proceedings of the 29th International Conference on Ocean, Offshore Mechanics and Artic Engineering; 2010.
13. Philstar Global, Available online: https://www.philstar.com/business/science-and-environment /2016/08/18/1614467/marine-scientist-eyes-rd-ocean-energy (Accessed 20 May, 2022)

14. Quirapas M.A.J.R., Lin H., Abundo M.L.S., Brahim S., Santod D. "Ocean renewable energy in Southeast Asia: A review" Renewable and Sustainable Energy Development 41 (2015) 799 – 817., https://doi.org/10.1016/j.rser.2014.08.016
15. MetOceanView. Available online: https://www.metoceanview.com/hindcast
16. PAGASA National meteorological, hydrological and astronomical service agency of the Philippines. Available online: https://bagong.pagasa.dost.gov.ph/index.php
17. Municipality of Cuyo, Province of Palawan. Available online: https://philatlas.com/luzon/mimaropa/palawan,cuyo.html
18. Municipality of Magsaysay, Province of Palawan. Available online: https://philatlas.com/luzon/mimaropa/palawan.magsaysay.html
19. Blechenger P., Ermino R., Lopez A. Serafica E., Terrado E. "Solar hybridization of large-scale NPC-SPUG diesel power plants: A programmatic approach" European Union – Philippines Access to Sustainable Energy Program, June 22, 2018. Available online: https://www.eu-asep.ph/wp-content/uploads/2018/06/Solar-hybridization-of-large-scale-NPC-SPUG-diesel-power-plants-Programmatic-Approach-by-Philipp-Blechinger-PhD.pdf (Accessed 20, May 2022)
20. USACE Coastal Engineering Manual, 2002. Available online: https://www.publications.usace.army.mil/USACE-Publications/Engineer-Manuals/u43544q/636F617374616C20656E67696E656572696E67206D616E75616C/
21. Pacaldo, J. C., Abundo, M. L. S., Billotindos, L. M., & Baco Jr, C. S. (2022). Performance Analysis of a Hybrid Diesel–Renewable Energy (RE) Electrical System in Cuyo Island, Palawan, Philippines. International Journal of Advanced Research in Engineering Innovation, 4(1), 1-15., https://doi.org/10.55057/ijarei.2022.4.1.1
22. McComb, P. J., & Johnson, D. L. (2011). A high-resolution weather forecasting tool for marine operations management in ports and harbours. Proceedings of Coast and Ports. Available online: https://citeseerx.ist.psu.edu/viewdoc/download?doi=10.1.1.473.2202&rep=rep1&type=pdf (Accessed 23 May, 2022)
23. Boulay, S. O., & Batt, L. (2015, January). Marine weather forecasting and monitoring at the Port of Sydney and Botany Bay, NSW, Australia. In Proceedings of the Australasian Coasts & Ports Conference (p. 102). Available online: https://www.researchgate.net/profile/Sebastien-Boulay/publication/283824032_Marine_weather_forecasting_and_monitoring_at_the_Port_of_Sydney_and_Botany_Bay_NSW_Australia/links/564812b208ae9f9c13e97f3b/Marine-weather-forecasting-and-monitoring-at-the-Port-of-Sydney-and-Botany-Bay-NSW-Australia.pdf
24. David J. Sanderson, David C.P. Peacock, Making rose diagrams fit-for-purpose, Earth-Science Reviews, Volume 201, 2020, 103055, ISSN 0012-8252, https://doi.org/10.1016/j.earscirev.2019.103055.
25. Bryant, M.A., Hesser, T.J., & Jensen, R.E. (2016). Evaluation statistics computed for the Wave Information Studies (WIS). Available online: https://apps.dtic.mil/sti/pdfs/AD1013235.pdf (Accessed 23 May, 2022)
26. Akpınar, A., & Kömürcü, M. İ. (2013). Assessment of wave energy resource of the Black Sea based on 15-year numerical hindcast data. *Applied Energy*, *101*, 502-512. https://doi.org/10.1016/j.apenergy.2012.06.005
27. Booij, N., Ris, R. and Holthuijsen, L. (1999) A Third-Generation Wave Model for Coastal Regions. I—Model Description and Validation. Journal of Geophysical Research, 104, 7649-7666. https://doi.org/10.1029/98JC02622.
28. Bento, A. R., Martinho, P., & Soares, C. G. (2018). Wave energy assessment for Northern Spain from a 33-year hindcast. *Renewable Energy*, *127*, 322-333. https://doi.org/10.1016/j.renene.2018.04.049
29. Yang, Z., Shao, W., Ding, Y., Shi, J., & Ji, Q. (2020). Wave simulation by the SWAN model and FVCOM considering the sea-water level around the Zhoushan islands. *Journal of Marine Science and Engineering*, *8*(10), 783. https://doi.org/10.3390/jmse8100783
30. Silander, M. F. C., & Moreno, C. G. G. (2019). On the spatial distribution of the wave energy resource in Puerto Rico and the United States Virgin Islands. Renewable Energy, 136, 442-451. https://doi.org/10.1016/j.renene.2018.12.120
31. Rusu, E., & Soares, C. G. (2012). Wave energy pattern around the Madeira Islands. *Energy*, *45*(1), 771-785. https://doi.org/10.1016/j.energy.2012.07.013
32. Buonaiuto Jr, F. S., Slattery, M., & Bokuniewicz, H. J. (2011). Wave modeling of Long Island coastal waters. Journal of Coastal Research, 27(3), 470-477. https://doi.org/10.2112/08-1014.1
33. Stopa, J. E., Filipot, J. F., Li, N., Cheung, K. F., Chen, Y. L., & Vega, L. (2013). Wave energy resources along the Hawaiian Island chain. *Renewable Energy*, *55*, 305-321. https://doi.org/10.1016/j.renene.2012.12.030
34. Rusu, L., & Soares, C. G. (2012). Wave energy assessments in the Azores islands. *Renewable Energy*, *45*, 183-196. https://doi.org/10.1016/j.renene.2012.02.027
35. Bernardino, M., Rusu, L., & Soares, C. G. (2017). Evaluation of the wave energy resources in the Cape Verde Islands. Renewable Energy, 101, 316-326. https://doi.org/10.1016/j.renene.2016.08.040
36. Rezaei, F., Tajziehchi, M., Soltanpour, M., & Emami, A. (2014). Prediction of wave characteristics in Persian Gulf within Qeshm and Hormoz Islands using swan wave model. International Conference on Coasts, Ports and marine Structures, November 2014. Available online: https://www.researchgate.net/publication/329327272_PREDICTION_OF_WAVE_CHARACTERISTICS_IN_PERSIAN_GULF_WITHIN_QESHM_AND_HORMOZ_ISLANDS_USING_SWAN_WAVE_MODEL. (Accessed 25 May, 2022)
37. Wu, Z., Chen, J., Jiang, C., & Deng, B. (2021). Simulation of extreme waves using coupled atmosphere-wave modeling system over the South China Sea. *Ocean Engineering*, *221*, 108531. https://doi.org/10.1016/j.oceaneng.2020.108531
38. Onea, F., & Rusu, L. (2015, May). Coastal impact of a hybrid marine farm operating close to the Sardinia Island. In *OCEANS 2015-Genova* (pp. 1-7). IEEE. Available online: https://tethys.pnnl.gov/publications/coastal-impact-hybrid-marine-farm-operating-close-sardinia-island (Accessed on 25 May, 2022)

39. Kompor, W., Tanaka, H., Ekkawatpanit, C., & Kositkittiwong, D. (2016). Application of simulating waves nearshore (swan) model for wave simulation in Gulf of Thailand. *Northeast. Reg. Disaster Sci. Res*, *52*, 139-144.
40. van Nieuwkoop, J. C., Smith, H. C., Smith, G. H., & Johanning, L. (2013). Wave resource assessment along the Cornish coast (UK) from a 23-year hindcast dataset validated against buoy measurements. *Renewable energy*, *58*, 1-14. https://doi.org/10.1016/j.renene.2013.02.033
41. Gonçalves, M., Martinho, P., & Soares, C. G. (2018). A 33-year hindcast on wave energy assessment in the western French coast. *Energy*, *165*, 790-801. https://doi.org/10.1016/j.energy.2018.10.002
42. Lavidas, G., Venugopal, V., & Friedrich, D. (2017). Wave energy extraction in Scotland through an improved nearshore wave atlas. *International Journal of Marine Energy*, *17*, 64-83. https://doi.org/10.1016/j.ijome.2017.01.008
43. Folley, M., & Whittaker, T. J. T. (2009). Analysis of the nearshore wave energy resource. *Renewable energy*, *34*(7), 1709-1715. https://doi.org/10.1016/j.renene.2009.01.003
44. Lucero, F., Catalán, P. A., Ossandón, Á., Beyá, J., Puelma, A., & Zamorano, L. (2017). Wave energy assessment in the central-south coast of Chile. *Renewable Energy*, *114*, 120-131. https://doi.org/10.1016/j.renene.2017.03.076
45. Cuttler, M. V., Hansen, J. E., & Lowe, R. J. (2020). Seasonal and interannual variability of the wave climate at a wave energy hotspot off the southwestern coast of Australia. *Renewable Energy*, *146*, 2337-2350. https://doi.org/10.1016/j.renene.2019.08.058
46. GEBCO 2021, Available online: https://www.gebco.net/data_and_products/gridded_bathymetry_data/gebco_2021.html
47. Komen, G., Hasselmann, S., & Hasselmann, K. (1984). On the existence of a fully developed wind – sea spectrum. Journal of Physical Oceanography, 14, 1271, 1271 – 1285. https://doi.org/10.1175/1520-0485(1984)014<1271:OTEOAF>2.0.CO;2
48. Hasselmann, K., Barnett, T., Bouws, E., Carlson, H., Cartwright, D., Enke, K., … Walden, H. (1973). Measerements of wind wave growth and swell decay during the Joint North Sea Wave Project (JONSWAP). Deutsche Hydrographische Zeitschrift, 8, 12.
49. Guillou, N., & Chapalain, G. (2018). Annual and seasonal variabilities in the performances of wave energy converters. *Energy*, *165*, 812-823. https://doi.org/10.1016/j.energy.2018.10.001
50. Vannucchi, V., & Cappietti, L. (2016). Wave energy assessment and performance estimation of state of the art wave energy converters in Italian hotspots. *Sustainability*, *8*(12), 1300. https://doi.org/10.3390/su8121300
51. Johnson, H. K., & Kofoed-Hansen, H. (2000). Influence of bottom friction on sea surface roughness and its impact on shallow water wind wave modeling. *Journal of physical oceanography*, *30*(7), 1743-1756. https://doi.org/10.1175/1520-0485(2000)030<1743:IOBFOS>2.0.CO;2
52. Ponce de León, S., & Guedes Soares, C. (2005). On the sheltering effect of islands in ocean wave models. *Journal of Geophysical Research: Oceans*, *110*(C9). https://doi.org/10.1029/2004JC002682
53. Wan, Y., Zhang, J., Meng, J., & Wang, J. (2015). Exploitable wave energy assessment based on ERA-Interim reanalysis data—A case study in the East China Sea and the South China Sea. *Acta Oceanologica Sinica*, *34*(9), 143-155. https://doi.org/10.1007/s13131-015-0641-8
54. Mirzaei, A., Tangang, F., & Juneng, L. (2015). Wave energy potential assessment in the central and southern regions of the South China Sea. *Renewable Energy*, *80*(C), 454-470. https://doi.org/10.1016/j.renene.2015.02.005
55. Xia, G., Draxl, C., Raghavendra, A., & Lundquist, J. K. (2021). Validating simulated mountain wave impacts on hub-height wind speed using SoDAR observations. *Renewable Energy*, *163*, 2220-2230. https://doi.org/10.1016/j.renene.2020.10.127
56. Wang, Z., Dong, S., Dong, X., & Zhang, X. (2016). Assessment of wind energy and wave energy resources in Weifang sea area. *International Journal of Hydrogen Energy*, *41*(35), 15805-15811. https://doi.org/10.1016/j.ijhydene.2016.04.002